ERS-2 Wind Scatterometer Cyclic Report

from 24th May 1999 to 28th June 1999
Cycle 43

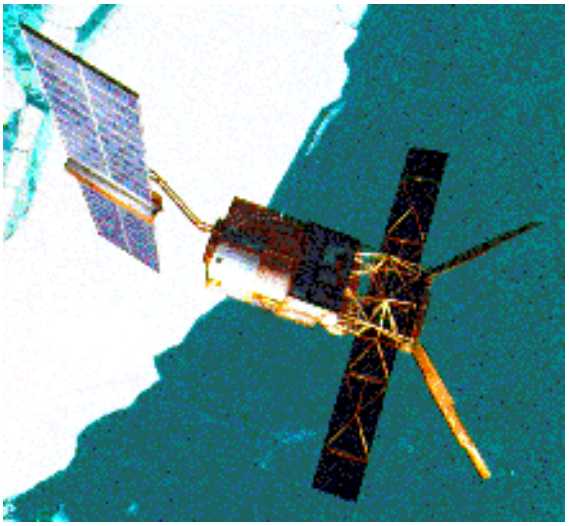

Prepared by:	PCS team	ESRIN APP-AEM
Inputs from:	F. Aidt	ESTEC TOS-EMS
	L. Isaksen	ECMWF

Document No: APP-AEM/PCS/WS99-005
Issue: 1.0
Date: 23rd, July 1999

Distribution List

ESAHQ	G. Duchossois	
	P. Martin	
ESTEC	M. Canela	APP-LR
	E. Attema	SCI-VRS
	F. Aidt	TOS-EMS
	B. Gelsthorpe	APP-LTP
	R. Zobl	
	K. van't Klooster	
ESOC	F. Bosquillon de Frescheville	TOS-OFC
	P. Jayaraman	TOS-OFC
ESRIN	M. Albani	APP-AE
	P. Lecomte	APP-AEM
	V. Beruti	APP-AEF
	S. D'Elia	APP-AEU
	G. Kohlhammer	APP-MMO
	U.Gebelein	Serco

L.A. Breivik	DNMI
P. Snoeij	DUT
J. Heidbreder	DORNIER
L. Isaksen	ECMWF
J. Kerkman, J. Figa	EUMETSAT
S. Pouliquen	F-PAF
V. Wismann	IFARS
A. Cavanie	IFREMER
R.S. Dunbar	JPL
A. Stoffelen	KNMI
G. Legg, P. Chang	NOAA/NESDIS
W. Gemmill	NOAA/NWS
J. Hawkins	NRL
D. Offiler, R. Graham, C.A. Parrette	UK-MET Office
F. Courtier, H. Roquet	Meteo-France
C. Scupniewicz	FNMOC
M. Stewart	University of Nottingham
R.A. Brown	University of Washington

This report and its annex are also available via FTP.
ftp pooh.esrin.esa.it (login as anonymous)
cd pub/SCATTEROMETER
wscatt_rep_43.ps.Z, annex_rep_43.ps.Z

1.0 Introduction and summary

The results reported in each section concern, apart from a summary of the daily quality control made within the PCS, the investigations and the study of "open-problems" related to the scatterometer, e.g. the CMOD-4 for high wind speed, the antenna pattern and so on.

In each section results are shown from the beginning of the mission in order to allow comparisons and to outline possible "seasonal" effects. An explanation of the major events that have impacted the performance since launch is given, and a comment about the recent events during the last cycle is included.

This report takes care of the period from 24th May 1999 to 28th June 1999 (cycle 43)

This report and its annex (the ECMWF reports) are available via ftp (login as anonymous) to the address pooh.esrin.esa.it directory /pub/SCATTEROMETER file names wscatt_rep_43.ps.Z, annex_rep_43.ps.Z (Unix compressed).

The availability of the ERS-2 Wind Scatterometer raw data during cycle 43 was 98.96% and the detailed list of the unavailability periods is available in the document "ERS-2 AMI/RA/ATSR/ GOME availability statistics" issued at the end of each cycle.

For the calibration performance the results are:

- The evolution of the maximum position of the gamma nought histograms computed over the rain forest is stable. On average the peak values for the aft and fore antenna are very close together, while for the mid antenna the peak value is roughly 0.2 dB less than the fore-aft case (in particular at descending passes from January 1999 onwards). A seasonal effect it also present in the peak position evolution for the three antennae.
- For cycle 43 the antenna patterns over the Brazilian rain forest (large area) are not available from ESTEC. The antenna patterns computed by PCS over a small area of the Brazilian rain forest are flat within 0.3 dB for both ascending and descending passes.The small slope at the near-mid range of the fore and aft antenna profiles (at descending passes) is still present.The mid antenna profile, at far range descending passes, is roughly 0.1-0.2 dB less than the fore and aft ones (as reported for cycle 43).
- The antenna patterns computed on the ocean (by ECMWF) are very similar to the ones of the previous cycle. The mid antenna profile shows a small slope from near range to far range that is not present in the antenna pattern computed over the rain forest.
- During the planned calibration passes the transponders were switched-off during the passage on 28th May 1999. For the other passages the transponders were switched-on but the gain constant values were not computed by ESTEC. The antenna patterns derived over the transponder are for this reason unchanged.
- The antenna temperature measured over the Brazilian rain forest during the cycle 43 confirms the increase of roughly 1 degree per year for the mid and fore antenna and roughly 2 degrees per year for the aft antenna. This increase in the antennae temperature could be related with the degradation of the antennae protection film.

For the instrument performance the results of the monitoring are:

- A decrease, during the cycle 43, of roughly 0.1 dB of the internal calibration level. This decrease is very similar to the one measured for cycle 42. Since 26th October 1998 (when 2.0 dB were added to the transmitter power) the internal calibration level had a decrease, of roughly 0.5 dB (for the three antennae): on average 0.07 dB per cycle. This decrease is less than the one reported before the increase of the transmitted power (0.1 dB per cycle).
- During the cycle 43 the monitoring of the dopppler compensation shows small differences with reference to the previous cycle. In particular the CoG of the fore antenna had an increase of roughly 40Hz (it was stable during the cycle 42), the CoG of the aft antenna had a decrease of roughly 40 Hz (while a small increase was reported for the cycle 42) and the CoG of the mid antenna still shows an increase. The standard deviation of the CoG was stable for the mid antenna while it had an increase in the case of the fore and aft antenna.
- The noise power has been affected by a period of instability from 7th June to 9th June 1999 in connection with the AMI anomaly occurred on 7th June. Apart from that period the evolution of the noise power was within the nominal value.

For the product performance the results are:

- During the cycle 43 the AMI instrument has been operated in scatterometer mode for 89.3% (ascending passes) and 82.0% (descending passes) of the total operation time (AMI unavailability, descoping and data lost are excluded). These values are very similar to the ones of cycle 42.
- During the cycle 43 there was an improvement in the scatterometer coverage of the west coast of the Mexico at descending passes. The west coast of Mexico is an important area to monitoring the formation of the tropical cyclones and scatterometer data are very useful into the forecast of these natural events (as reported by the ASCATT-SAG members). The improvement is due to the reduction of the length of the SAR segment acquired over the east coast of the USA. The length of the SAR images, over the east coast of USA, are now strictly limited to the length requested by the users.
- For cycle 43 the PCS quality control has reported stable results apart from the day 21st June 1999 when the operational set of meteo tables was missing into the ground station of Gatineau. This caused an ambiguity removal rate around 82% for that day. The number of valid sigma-nought triplets is roughly 160,000 per day The wind direction deviation is within -90.0, +90.0 degrees for 93% of the nodes, the ambiguity removal works successfully for 90% of the nodes. For cycle 43 the wind speed bias ranges from 0.1m/s to -0.4 m/s with a standard deviation of 2.5 m/s.
- The ECMWF reports, attached as annex, presents stable performances in the monitoring of the ERS-2 wind for the cycle 43. The wind speed bias is roughly -0.43 m/s for the UWI-FG analysis and -0.17 m/s for the FG-4D-Var case with a standard deviation of 1.56 m/s (UWI-FG) and 1.67 m/s (FG-4D-Var). The wind direction standard deviation is between 30 and 65 degrees (UWI - FG) or 15 and 30 degrees (FG-4D-Var). These results are very similar to the ones obtained in the previous report

2.0 Calibration Performances

The calibration performances are estimated using three types of target: a man made target (the transponder) and two natural targets (the rain forest and the ocean). This approach allow us to design the correct calibration using a punctual but accurate information from transponders and an extended but noisy information from rain forest and ocean for which the main component of the variance comes from the geophysical evolution of the natural target and from the backscattering models used. These aspects are in the calibration performance monitoring philosophy. The major goals of the calibration monitoring activities are the achievement of a “flat” antenna pattern profile and the assurance of a stable absolute calibration level.

2.1 Gain Constant over transponder

One gain constant is computed per transponder per beam from the actual and simulated two-dimensional echo power, which is given as a function of the orbit time and range time. This parameter clearly indicates the difference between “real instrument” and the mathematic model. In order to acquire data over the transponder the Scatterometer must be set into an appropriate operational mode that is defined as “Calibration”.

Table 1 shows the result of the calibration plan for cycle 43. The “Yes” in the EWIC column means that the raw data are available, “No” means the opposite case. The “On” in the transponder status column means that, from the raw data (EWIC), the transponders has been recognised as switched-on; “Off” means the opposite case. The “Yes” in the GC computed column means that a gain constant value has been retrieved, “No” means the opposite case.

For the cycle 43 no inputs were received by ESTEC.

TABLE 1. Calibration Plan: Summary Cycle 43

DATE	ORBIT (absolute)	ORBIT (relative)	Passage	Ground Station	EWIC (raw data)	AMI mode	Transponder Status	GC computed
990525	21670	8	D	KS	Yes	Calibration	On	No
990528	21713	51	D	KS	Yes	Calibration	Off	n/a
990613	21405	273	A	MS	Yes	Calibration	On	No
990615	21448	316	A	MS	Yes	Calibration	On	No

Figure 1 and Figure 2 show the gain constants available since the beginning of the mission, the analysis is split for the different antenna elevation angle. From these figure it is clear that the gain constant measurements are stable (within +/-0.5 dB) but after the end of the commissioning phase (cycle 11) only few data are available.

The plots in Figure 3 show the value of the Gain Constant for the three beams and for the ascending, descending and all passes. The plots show the average of all gain constant available since January 1996 (cycle 8) for each antenna elevation angle. The antenna patterns are flat but there is a clear shift of the level of the curves. On average, the mid beam is 0.3 dB higher than the aft one

and 0.5 dB higher than the fore one. For the descending passes the antenna pattern shows a slight slope from far range to near range.

Since September 1996 ESTEC has added a scaling factor to the gain constant in order to remove the bias among the three antennae. The gain constants were increased by 0.2 dB, -0.3 dB and 0.2 dB, for the fore, mid and aft beam respectively. The result is shown in figure 4. The suggestion given by ESTEC has not been introduced into the ground processing because the antenna patterns computed over the rain forest do not show such bias (see Figure 5). So in the actual scenario, the differences among the antennae are considered as a bias due to the transponder themselves.

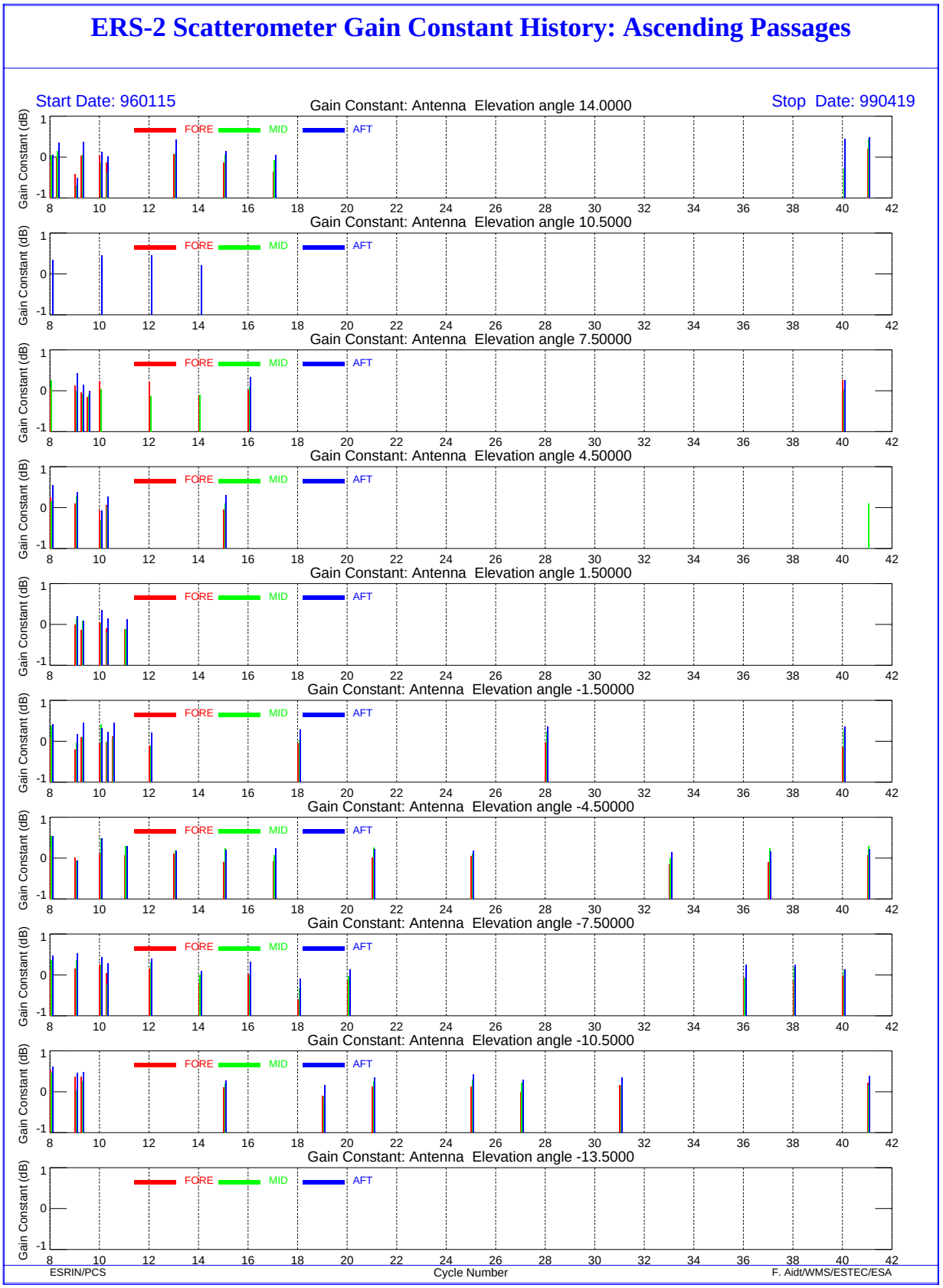

FIGURE 1. ERS-2 Scatterometer; gain Constant over transponder since the beginning of the mission (ascending passes).

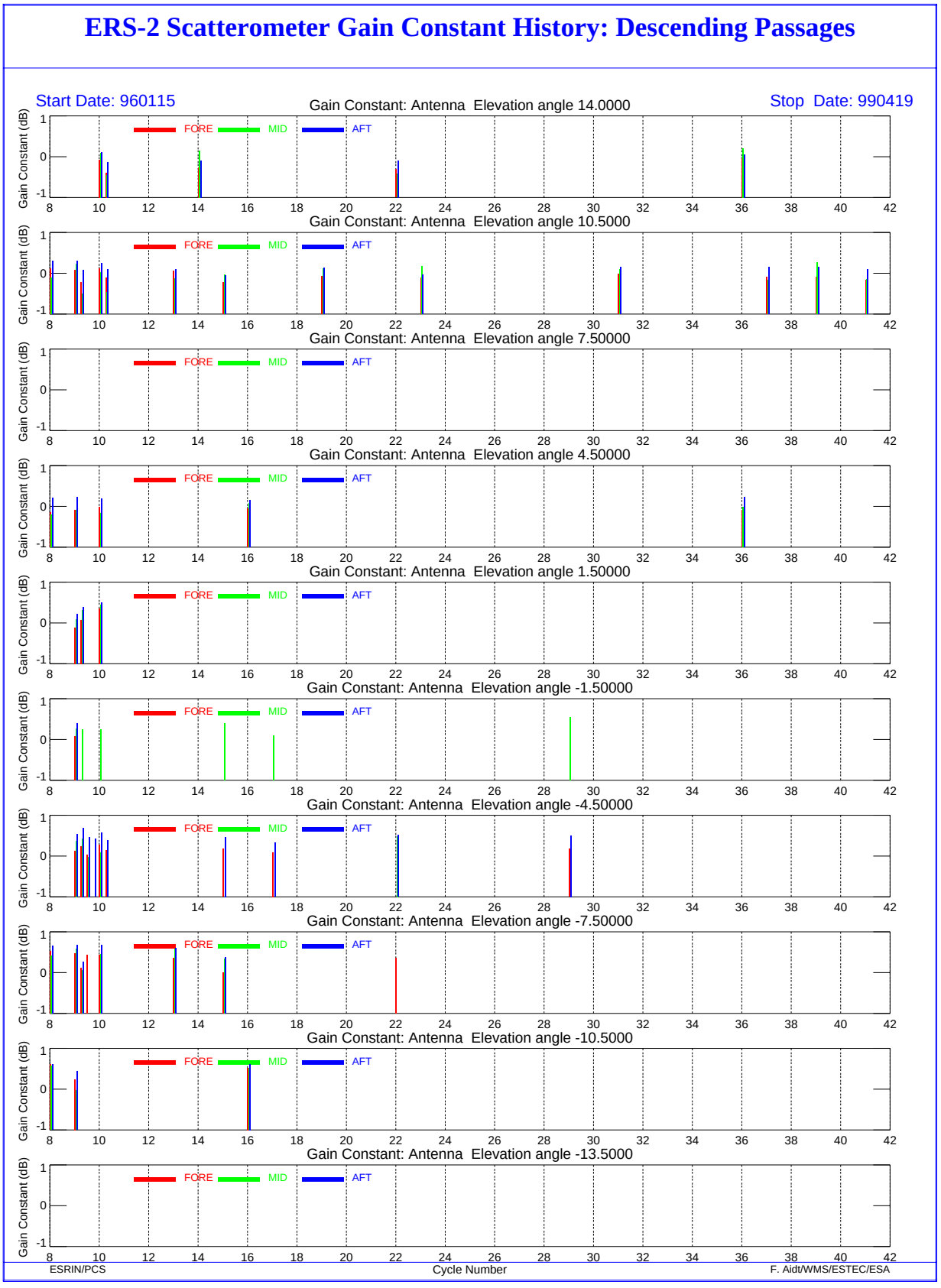

FIGURE 2. Scatterometer; gain Constant over transponder since the beginning of the mission (descending passes)

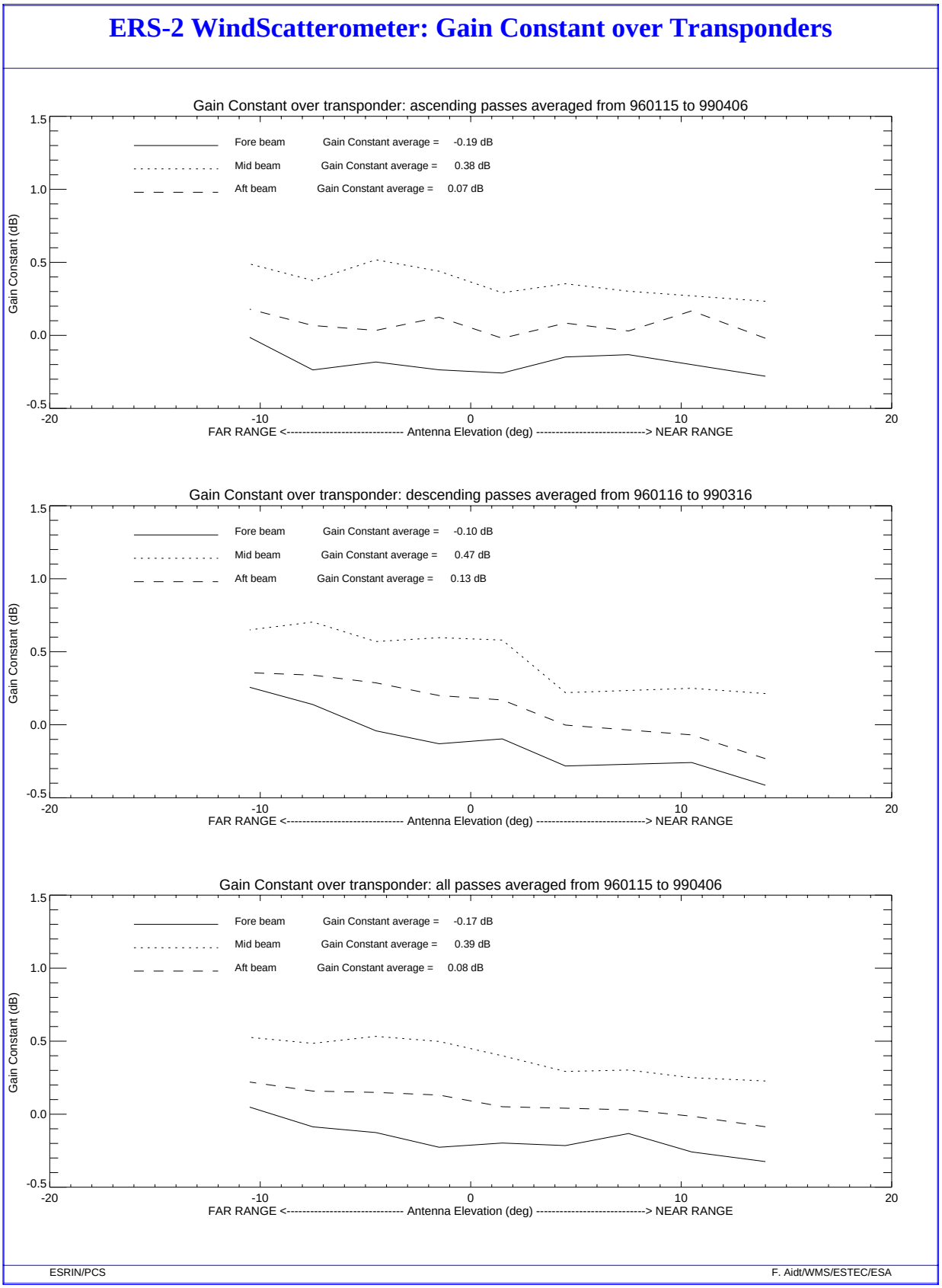

FIGURE 3. ERS-2 Scatterometer: gain constant over transponders. All data available since January 1996. Upper plot: ascending passes. Middle plot: descending passes. Lower plot: all passes.

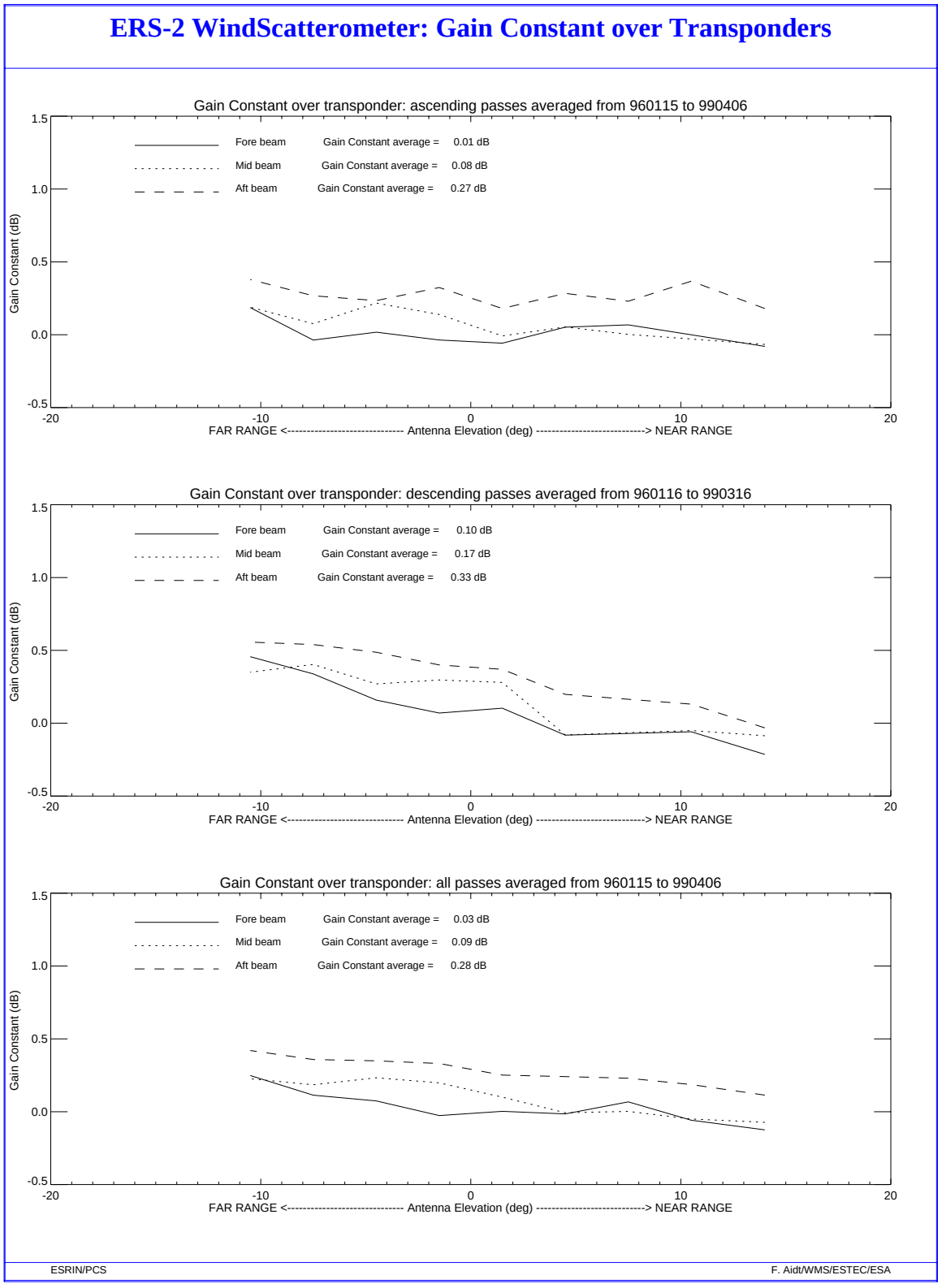

FIGURE 4. ERS-2 Scatterometer: gain constant over transponders plus a scaling factor. All data available since January 1996. Upper plot: ascending passes. Middle plot: descending passes. Lower plot: all passes.

2.2 Ocean Calibration

ECMWF performs the monitoring of ERS-2 sigma noughts over ocean (see the report in Annex).

For the cycle 43 the sigma nought bias, defined as the difference between the ERS-2 sigma-nought and the sigma nought retrieved using the CMOD-4 model with the First Guess at Appropriate Time (FGAT) background, has ranged from 0.2 dB to 0.3 dB for the incidence angle above 32 degrees. This result is very close to the one reported for the previous cycle.

It is important to underline that this bias rose on September 1997 when the ECMWF monitoring scheme was slightly changed (see report for cycle 25th from September 1st, 1997 to October 5th 1997). With this upgrade, the wind retrieval has also been improved, with a refined bias corrected version of CMOD4. In the monitoring of the sigma noughts the new version of CMOD4 has not been taken into account, so it is still performed against model sigma nought's simulated with the standard version of CMOD4.

The shape of the antenna patterns are very close to the ones obtained for the previous cycle. There is a small slope (from near range to far range) in the mid antenna's profile while the aft and fore antenna's profiles are very flat (in particular for the descending passes).

2.3 Gamma-nought over Brazilian rain forest

Although the transponders give accurate measurements of the antenna attenuation at particular points of the antenna pattern, they are not adequate for fine tuning across all incidence angles, as there are simply not enough samples. The tropical rain forest in South America has been used as a reference distributed target. The target at the working frequency (C-band) of ERS-2 Scatterometer acts as a very rough surface, and the transmitted signal is equally scattered in all directions (the target is assumed to follow the isotropic approximation). Consequently, for the angle of incidence used by ERS-2 Scatterometer, the normalised backscattering coefficient (sigma-nought) will depend solely on the surface effectively seen by the instrument:

$$S^0 = S \bullet \cos\theta$$

With this hypothesis it is possible to define the following formula:

$$\gamma^0 = \frac{\sigma^0}{\cos\theta}$$

Using this relation, the gamma-nought backscattering coefficient over the rain forest is independent of the incident angle, allowing the measurements from each of the three beams to be compared.

The test area used by the PCS is located between 2.5 degrees North and 5.0 degrees South in latitude and 60.5 degrees West and 70.0 degrees West in longitude.

The following paragraphs give a description of the activities carried out with this natural target.

2.3.1 Antenna pattern: Gamma-nought as a function of elevation angle

This analysis is carried out by ESTEC that has selected a larger region than the one used as test area within PCS. In this case the selected rain forest extends from 2.0 degrees South to 11.0 degrees South in latitude and 56.0 degrees West to 80 degrees West in longitude. A large area is selected in order to have a larger amount of measurements.

For cycle 43 the antenna patterns as function of the elevation angle have not been computed by ESTEC.

2.3.2 Antenna pattern: Gamma-nought as a function of incident angle

Figure 5 shows the antenna patterns as a function of the incident angle for cycle 43. The chosen Brazilian rain forest area, where the antenna patterns are computed, is the small one used by the PCS as test site to compute the weekly histograms.

The antenna patterns show a flat profile, within 0.3 dB for the ascending passes and within 0.5 dB for the descending ones. For the descending passes there is a small slope at the near-mid range of the fore and aft antenna profiles (as reported in the previous report).

The antenna profiles are very close together in particular at near range. For the descending passes the mid antenna profile at the far range is roughly 0.1-0.2 dB less than the fore and aft ones as reported in the previous report.

The mid antenna profiles doesn’t show the small slope reported in the case of ocean calibration.

The antenna profiles computed for the cycle 43 are very similar to the ones obtained for the cycle 42.

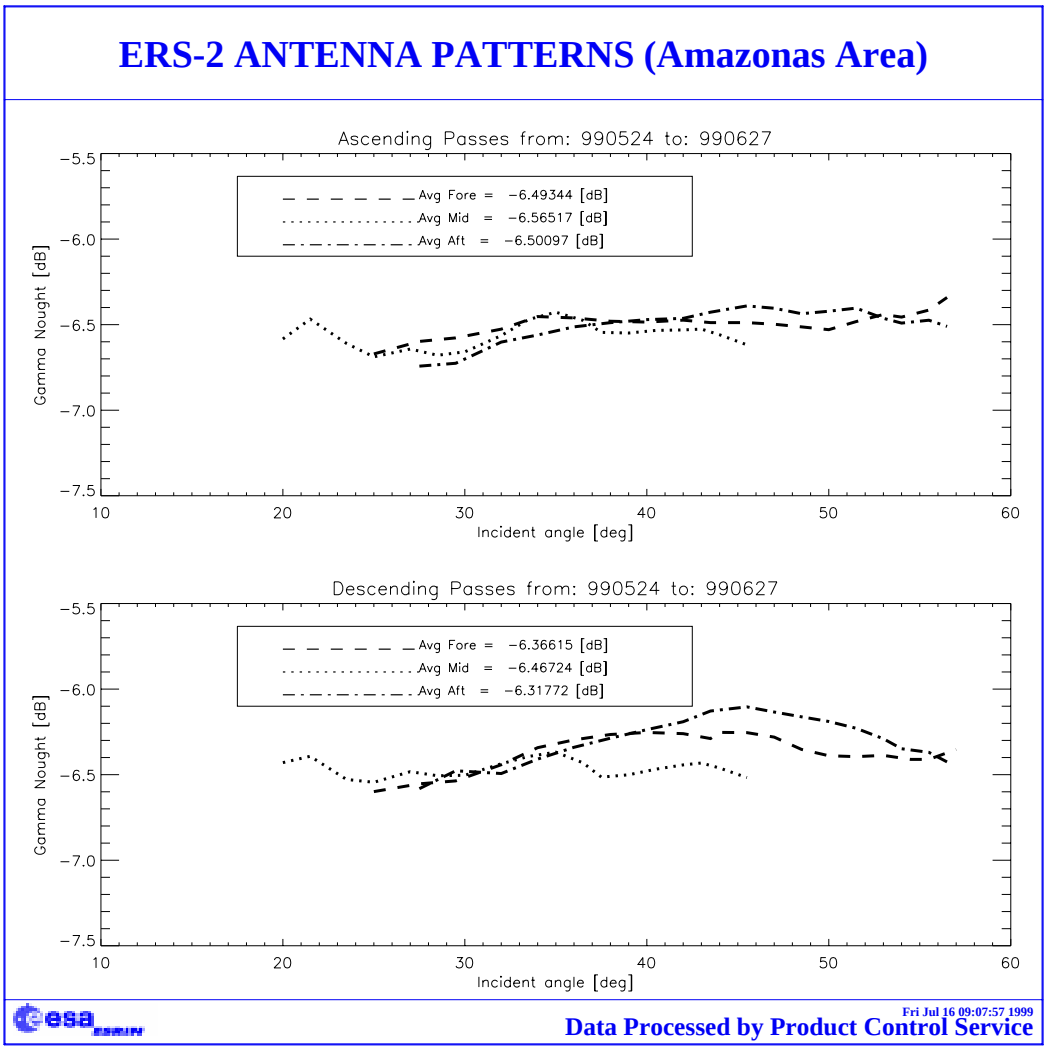

FIGURE 5. ERS-2 Scatterometer antenna patterns as function of the incident angle: cycle 43

2.3.3 Gamma-nought histograms and peak position evolution

As the gamma-nought is independent from the incidence angle, the histogram of gamma-noughts over the rain forest is characterised by a sharp peak. The time-series of the peak position gives some information on the stability of the calibration. This parameter is computed by fitting the histogram with a normal distribution added to a second order polynomial:

$$F\langle x\rangle = A_0 \cdot \exp\left(-\frac{z^2}{2}\right) + A_3 + A_4 \cdot x + A_5 \cdot x^2$$

where: $z = \dfrac{x - A_1}{A_2}$

The parameters are computed using a non linear least square method called “gradient expansion”. The position of the peak is given by the maximum of the function F(x). The histograms are computed weekly (from Monday to Sunday) for each antenna individually (“Fore”, “Mid”, and “Aft”) and for ascending and descending passage with a bin size of 0.02 dB.

Figure 6 shows the evolution of the histograms peak position since January 1996. The step shown in March 1996 is due to the end of commissioning phase when a new Look Up Table was used in the ground stations for WSCATT FD-products generation. It is interesting to note the decrease of roughly 0.2 dB from August 1996 to June 1997. This is linked to the switch of the Scatterometer calibration subsystem from side A to side B on 6th of August. The redundancy of side A device caused a little change in the calibration that was corrected on 19th June 1997 with a new calibration LUT used in the ground processing.

Figure 7 shows the evolution of the peak position corrected with the new calibration set also for the period from August 1996 to June 1997. From the plots in figure 7 it is clear that the calibration stability achieved over the rain forest is within 0.5 dB. On average the peak values for the aft and fore antenna are very close together, while for the mid antenna the peak value is roughly 0.2 dB less than the fore-aft case (in particular from the beginning of 1999 onwards). A seasonal effect it also present in the peak position evolution for the three antennae.

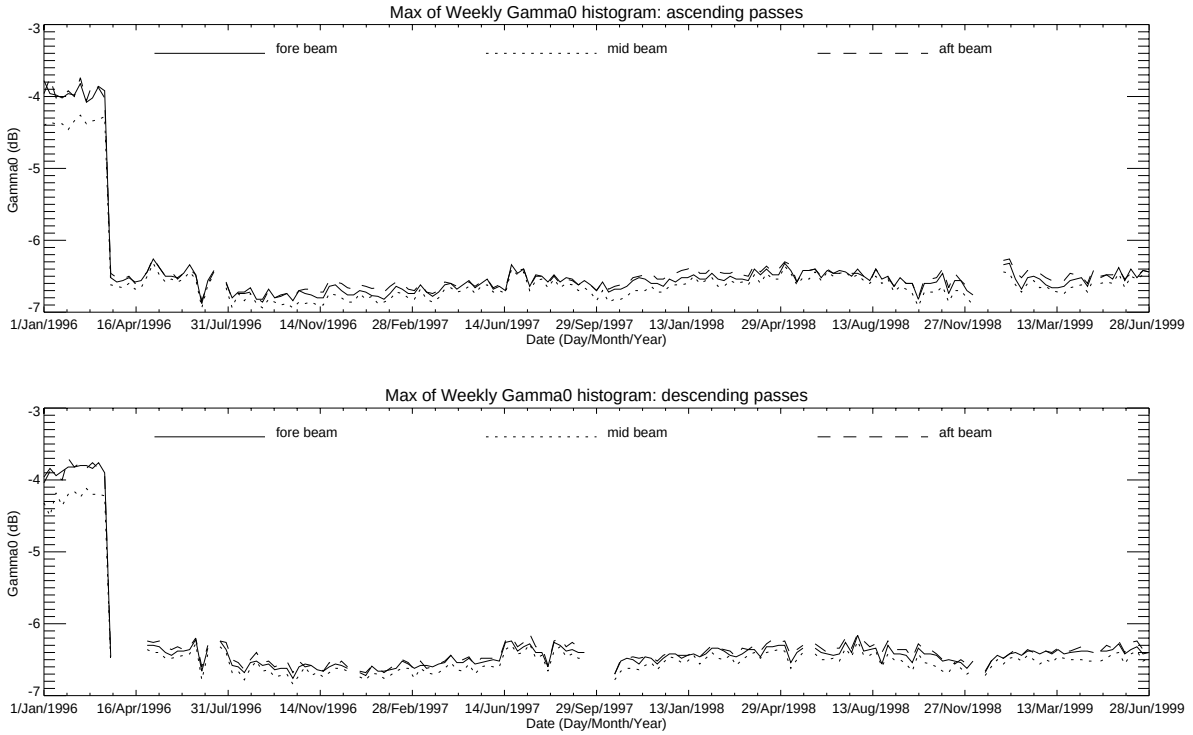

FIGURE 6. ERS-2 Scatterometer, gamma-nought histogram: weekly evolution of maximum position. From up to down: ascending passes, descending passes.

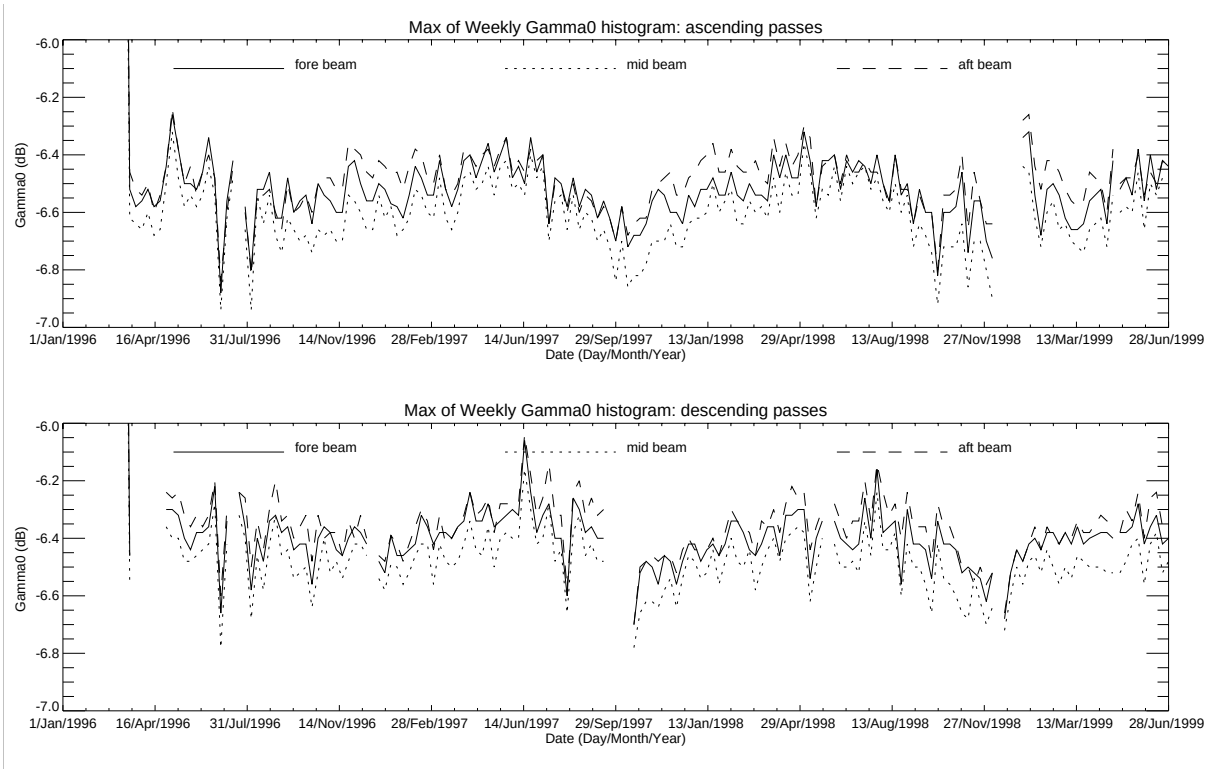

FIGURE 7. Gamma-nought histogram: weekly evolution of maximum position. Data from 6th of August 1996 to 19th June 1997 are corrected with the new calibration constant (+0.2dB). Upper plot: ascending passes. Lower plot: descending passes.

The mean and the standard deviation of gamma-nought are weekly computed directly using the Fast Delivery data. Figure 8 shows the evolution of the standard deviation since September 1996. The ascending passes show a gamma nought standard deviation more higher than the descending ones. This can be explained because at ascending passes the test site appears less homogeneous in particular for the some areas near the rivers (see Figure 14).

For the cycle 43 the evolution of the gamma nought standard deviation has been stable.

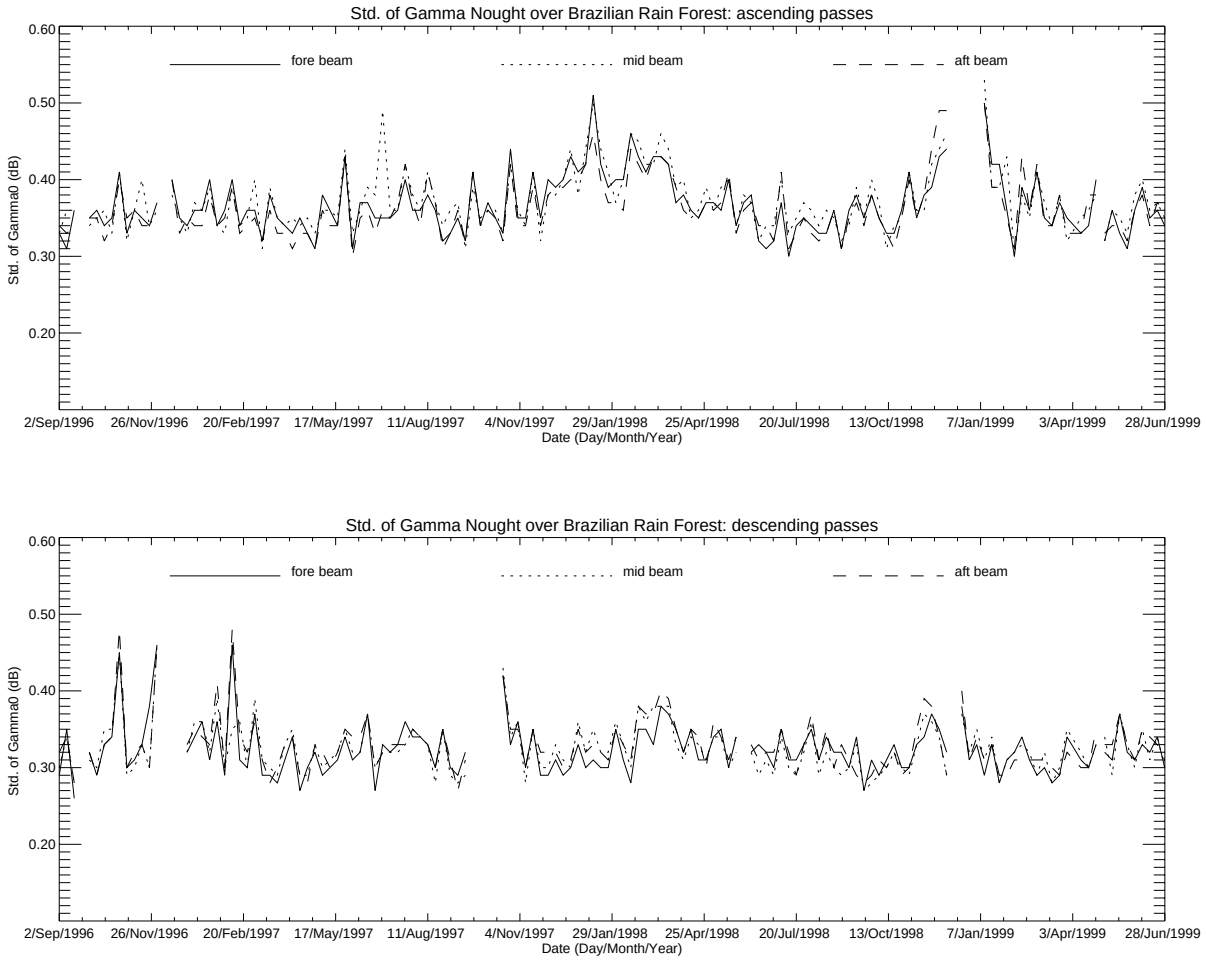

FIGURE 8. Gamma-nought histograms: weekly evolution of standard deviation. Upper plot: ascending pass. Lower plot descending pass.

The Figures from 9 to 13 show the gamma-nought histogram over the Brazilian rain forest throughout cycle 43.

The shape of the histograms has a good quality apart from the weeks 990607 (figure 11) and 990621 (figure 13) at ascending passes because a small amount of data is available. The histograms computed during the descending passes show a better quality in comparison with the histograms computed during the ascending passes.

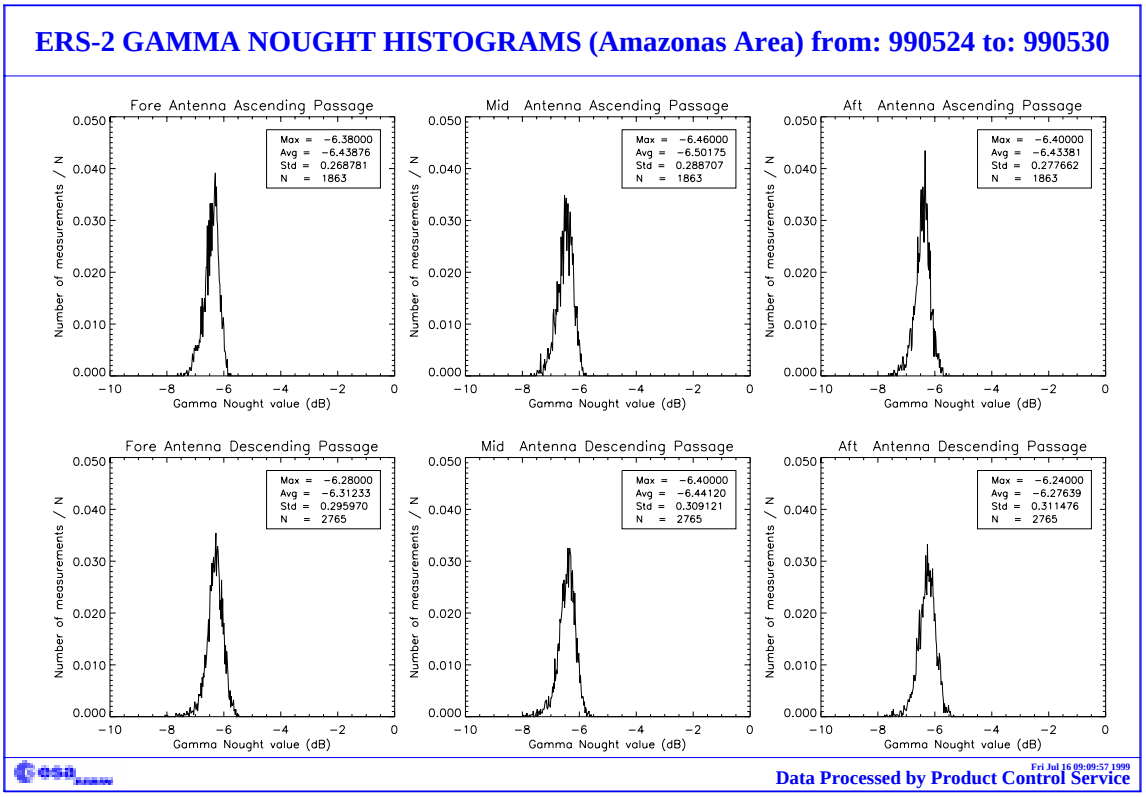

FIGURE 9. Gamma-nought histograms over Brazilian Rain forest: first week of the cycle.

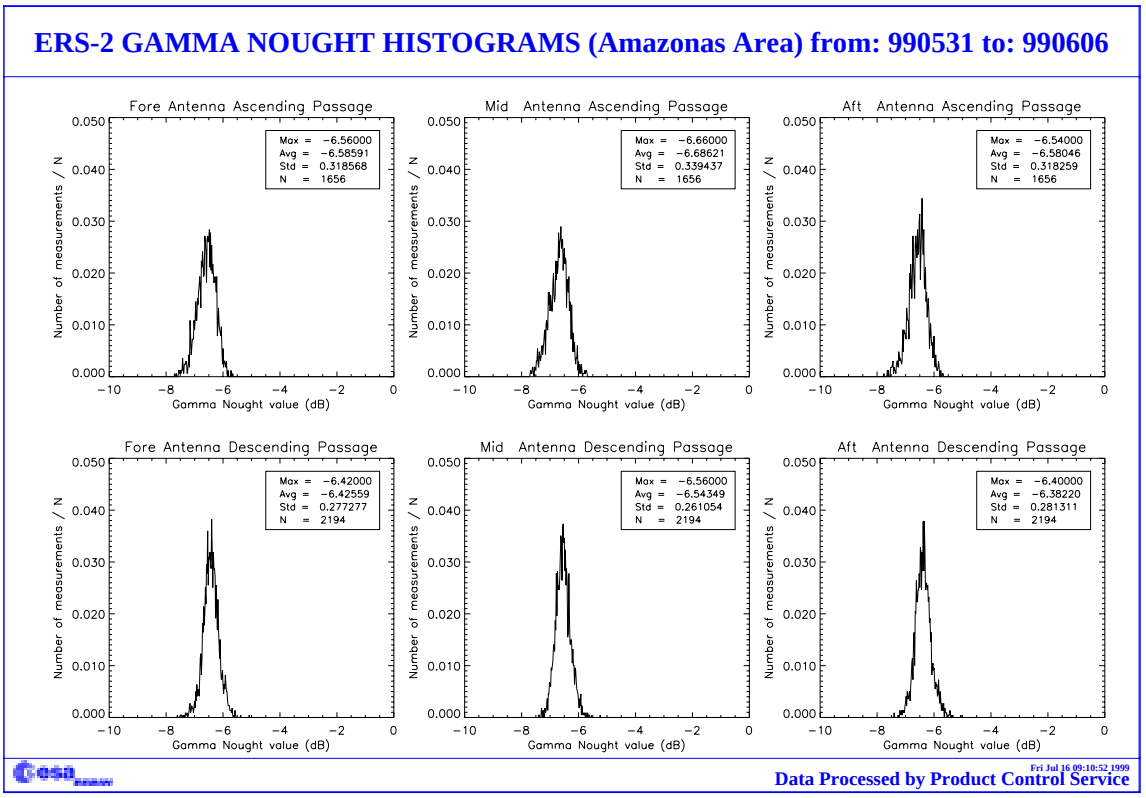

FIGURE 10. Gamma-nought histograms over Brazilian rain forest: second week of the cycle.

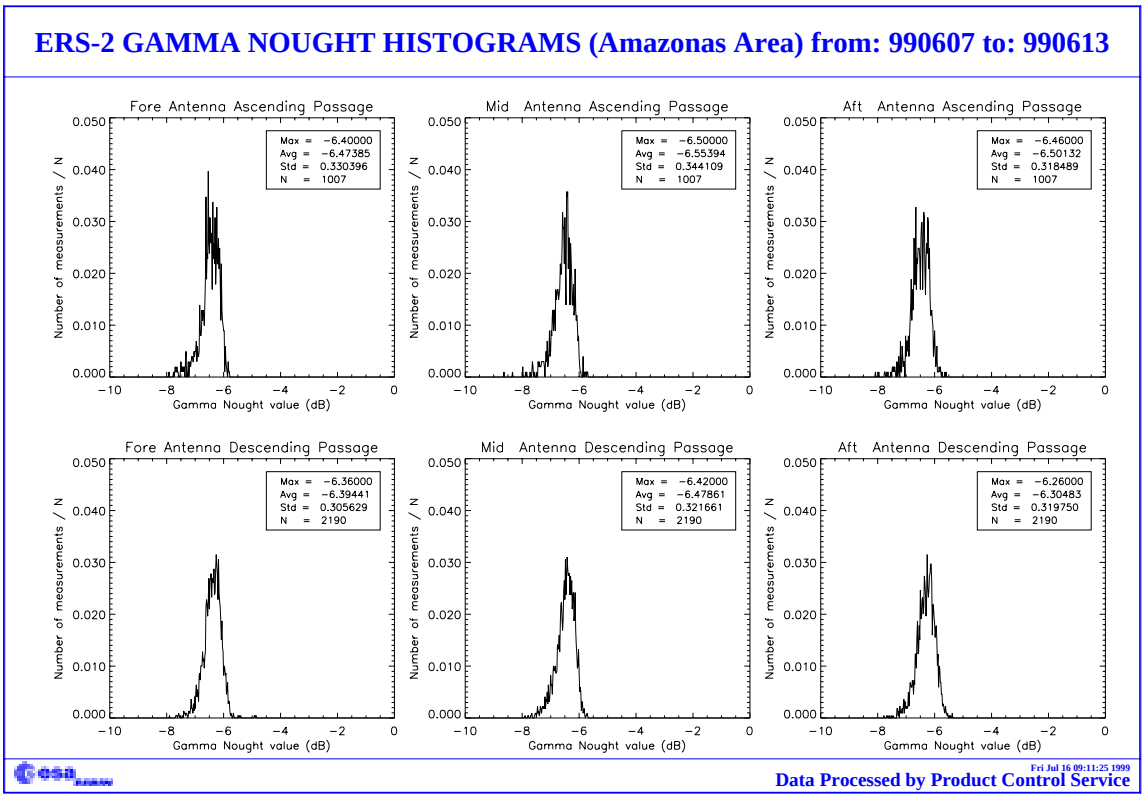

FIGURE 11. Gamma-nought histograms over Brazilian rain forest: third week of the cycle.

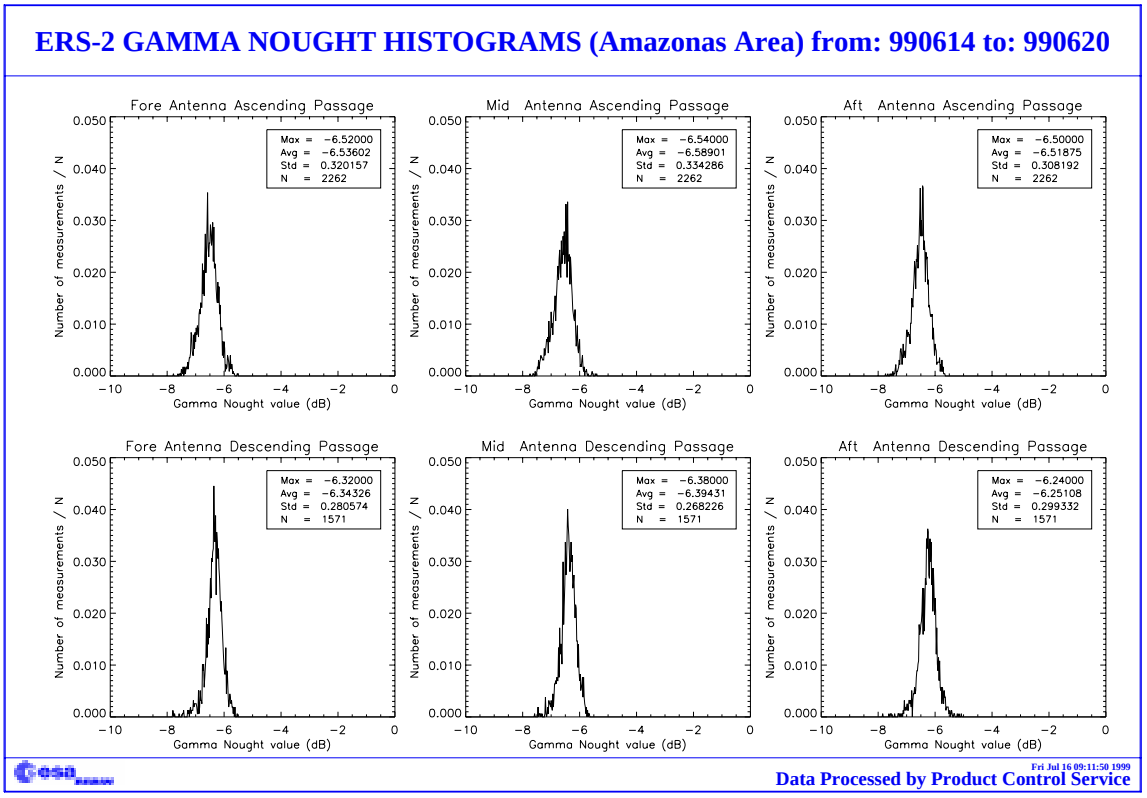

FIGURE 12. Gamma-nought histograms over Brazilian rain forest: fourth week of the cycle.

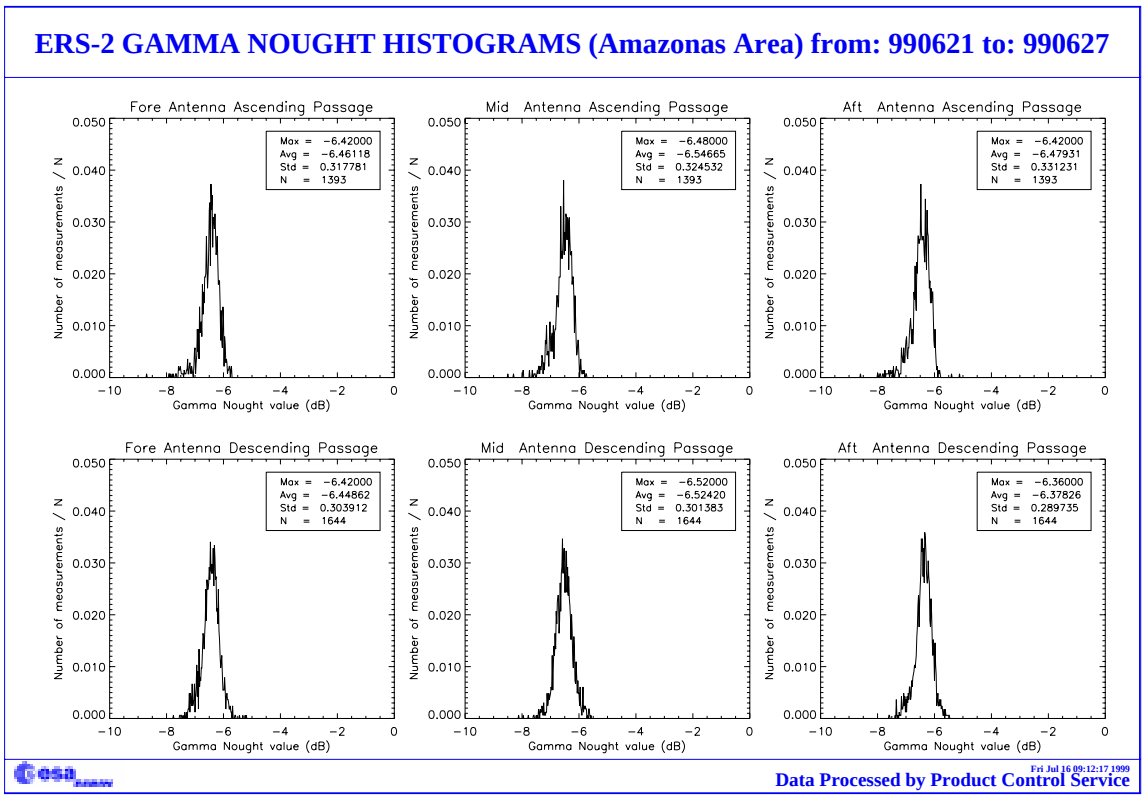

FIGURE 13. Gamma-nought histograms over Brazilian rain forest: fifth week of the cycle.

2.3.4 Gamma nought image of the reference area

The Figure 14 shows a map of the gamma nought (for cycle 43) over the Brazilian rain forest used as reference area within the PCS.

Each map has a resolution of 0.5 degrees in latitude and 0.5 degrees in longitude, roughly this is the instrument resolution at the latitude of the test site. In each resolution cell falls the average of all the valid observations available during one cycle (35 days).

From figure 14 it is clear that during the ascending passes the test area is less homogenous than in the descending ones. This seems due to the signal that comes from some areas near the rivers.

The set of images shown on Figure 14 is very similar to the one obtained for the previous cycle.

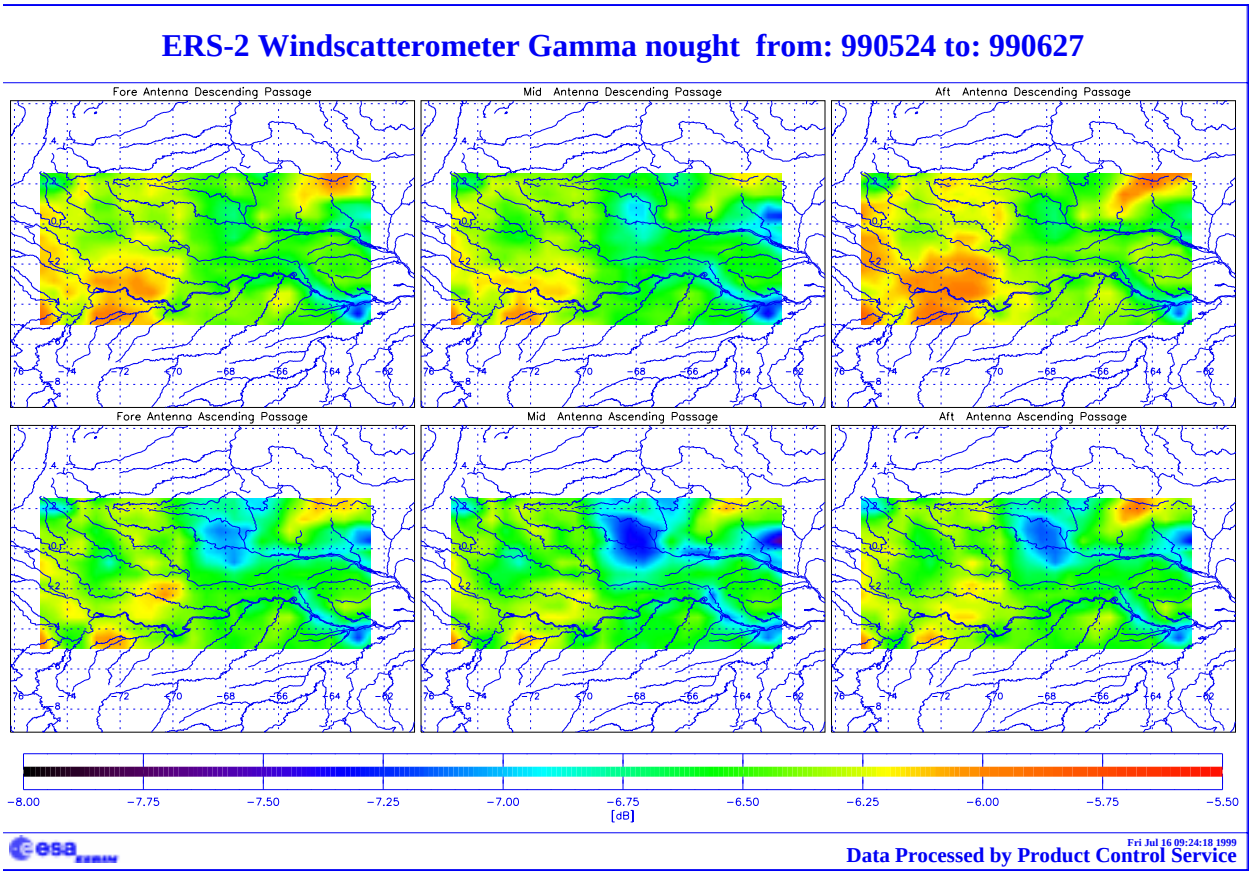

FIGURE 14. ERS-2 Scatterometer: gamma nought over the Brazilian rain forest cycle 43.

2.3.5 Antenna temperature evolution over the Rain Forest

The monitoring of the antenna temperature over the Brazilian rain forest is performed by PCS. The antenna temperatures are retrieved from the satellite telemetry when the Scatterometer swath is over the test site and the instrument is active (AMI in wind only or wind/wave mode). The scope of this monitoring is to investigate a possible correlation between the antenna temperatures and the gamma-nought level. This correlation is not clear in the actual data because of the gamma nought variability of the selected area. A deep analysis is to be performed to better understand the facts.

The plots for the three beams and for the ascending, descending and all passes are in Figure 15. It is interesting to note that the annual variation is due to the earth inclination and that the antenna temperatures have an increase of roughly 1.0 degree per year in the case of the mid and fore antenna; 2 degrees per year in the aft antenna's case.

This temperature increase could be related to the degradation of the antennae protection film.

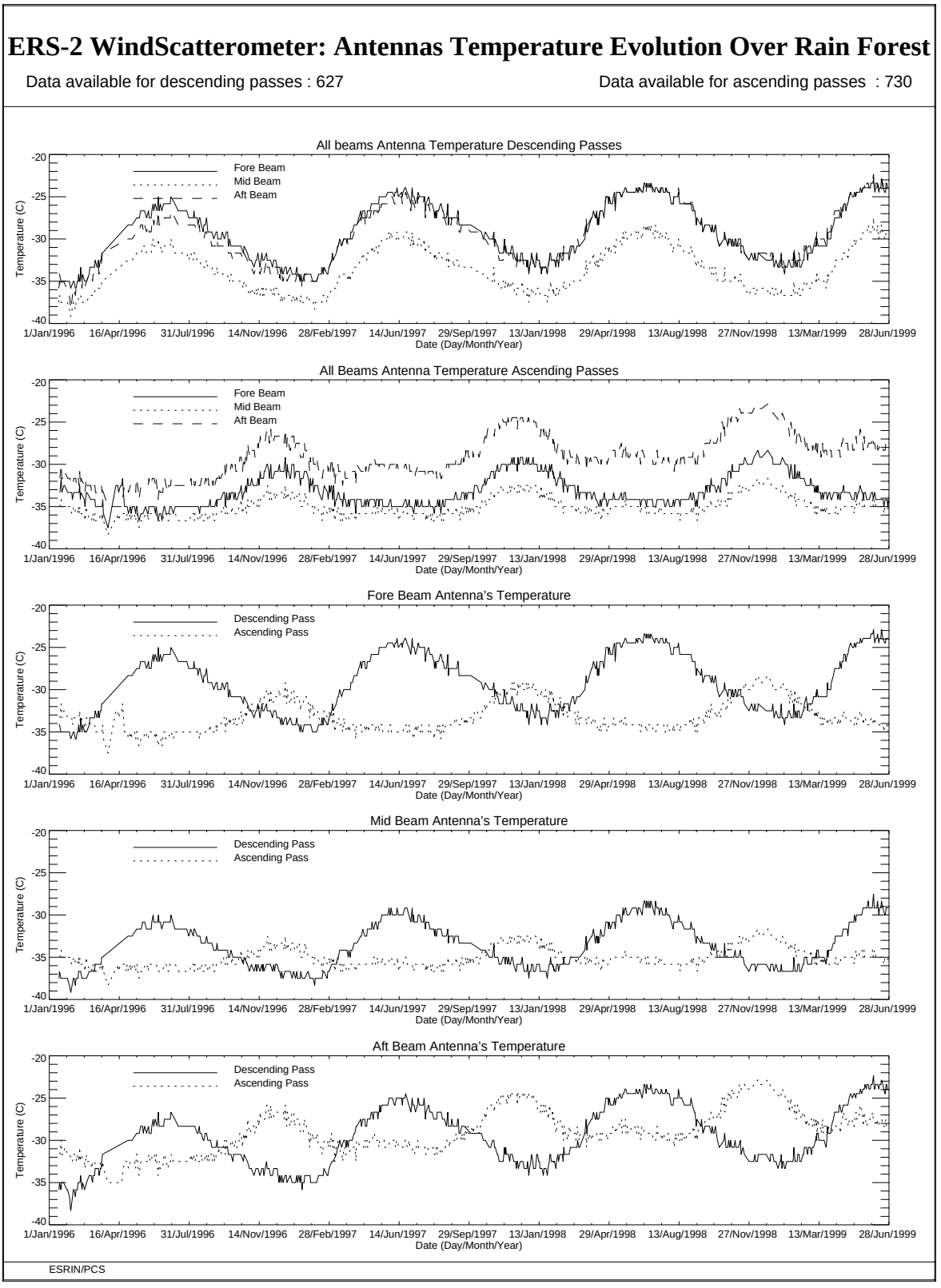

FIGURE 15. ERS-2 Scatterometer: evolution of the antenna temperatures over the Brazilian rain forest.

3.0 Instrument performance

The instrument status is checked by monitoring the following parameters:

- Centre of Gravity and standard deviation of the received signal spectrum. This parameter is useful for the monitoring of the orbit stability, the performances of the doppler compensation filter, the behaviour of the yaw steering mode and the performances of the devices in charge for the satellite attitude (e.g. gyroscopes, earth sensor).
- Noise power I and Q channel.
- Internal calibration pulse power.

the latter is an important parameter to monitor the transmitter and receiver chain, the evolution of pulse generator, the High Power Amplifier (HPA), the Travelling Wave Tube (TWT) and the receiver.

These parameters are extracted daily from the UWI products and averaged. The evolution of each parameter is characterised by a least square line fit. The coefficients of the line fit are printed in each plot

3.1 Centre of gravity and standard deviation of received power spectrum

The Figure 16 shows the evolution of the two parameters for each beam. The tendency since the beginning of the mission is a clear increase of the Centre of gravity (CoG) of the signal spectrum for the three antennae while the result for the standard deviation is more stable apart from the change occurred on 26th, October 1998. On October 26th, 1998 the standard deviation of the CoG had, on average, a decrease of roughly 100 Hz for the fore and aft antenna and of roughly 30Hz for the mid antenna. This change is linked with the increase of the transmitted power (see 3.3).

The two steps observed on the plots of the CoG (see Figure 16) are due to a change in the pointing subsystem (DES reconfiguration) side B instead of side A after a depointing anomaly (see table 2 for the list of the AOCS depointing anomaly occurred during the ERS-2 mission). The first change is from 24th, January 1996 to 14th, March 1996, the second one is from 14th February 1997 to 22nd April 1997. During these periods side B was switched on. It is important to note that during the first time a clear difference in the CoG is present only for the Fore antenna (an increase of roughly 100 Hz) while during the second time the change has affected all the three antennae (roughly an increase of 200 Hz, 50 Hz and 50 Hz for the fore, mid and aft antenna respectively).

Table 2: ERS-2 Scatterometer AOCS depointing anomaly

From	To
24th January 1996 9:10 a.m.	26th January 1996 6:53 p.m
14th February 1996 1:25 a.m.	15th February 1996 3:44 p.m
3rd June 1998 2:43 p.m.	6th June 1998 12:47 a.m.

The large deviations from the nominal values in the plots of the CoG of the fore and aft antenna are due to the missing of the Yaw Steering Mode or are due to the missing of the on board doppler coefficients as reported in Table 3.

Table 3: ERS-2 Scatterometer anomalies in the CoG fore and aft antenna

Date	Reason
26th and 27th September 1996	missing on-board doppler coefficient (after cal. DC converter test period)
6th and 7th June 1998	no Yaw Steering Mode (after depointing anomaly)
2nd and 3rd December 1998	missing on-board doppler coefficients (after AMI anomaly 228)

The peaks shown in the plot of mid beam CoG standard deviation are linked to the satellite manoeuvres and the DES reconfiguration.

During the cycle 43 the monitoring of the dopppler compensation shows small differences with reference to the previous cycle. In particular the CoG of the fore antenna had an increase of roughly 40Hz (it was stable during the cycle 42), the CoG of the aft antenna had a decrease of roughly 40 Hz (while a small increase was reported for the cycle 42) and the CoG of the mid antenna still shows an increase. The standard deviation of the CoG was stable for the mid antenna while it had an increase in the case of the fore and aft antenna. Figure 17 shows the evolution of the doppler compensation throughout the cycles 42 and 43.

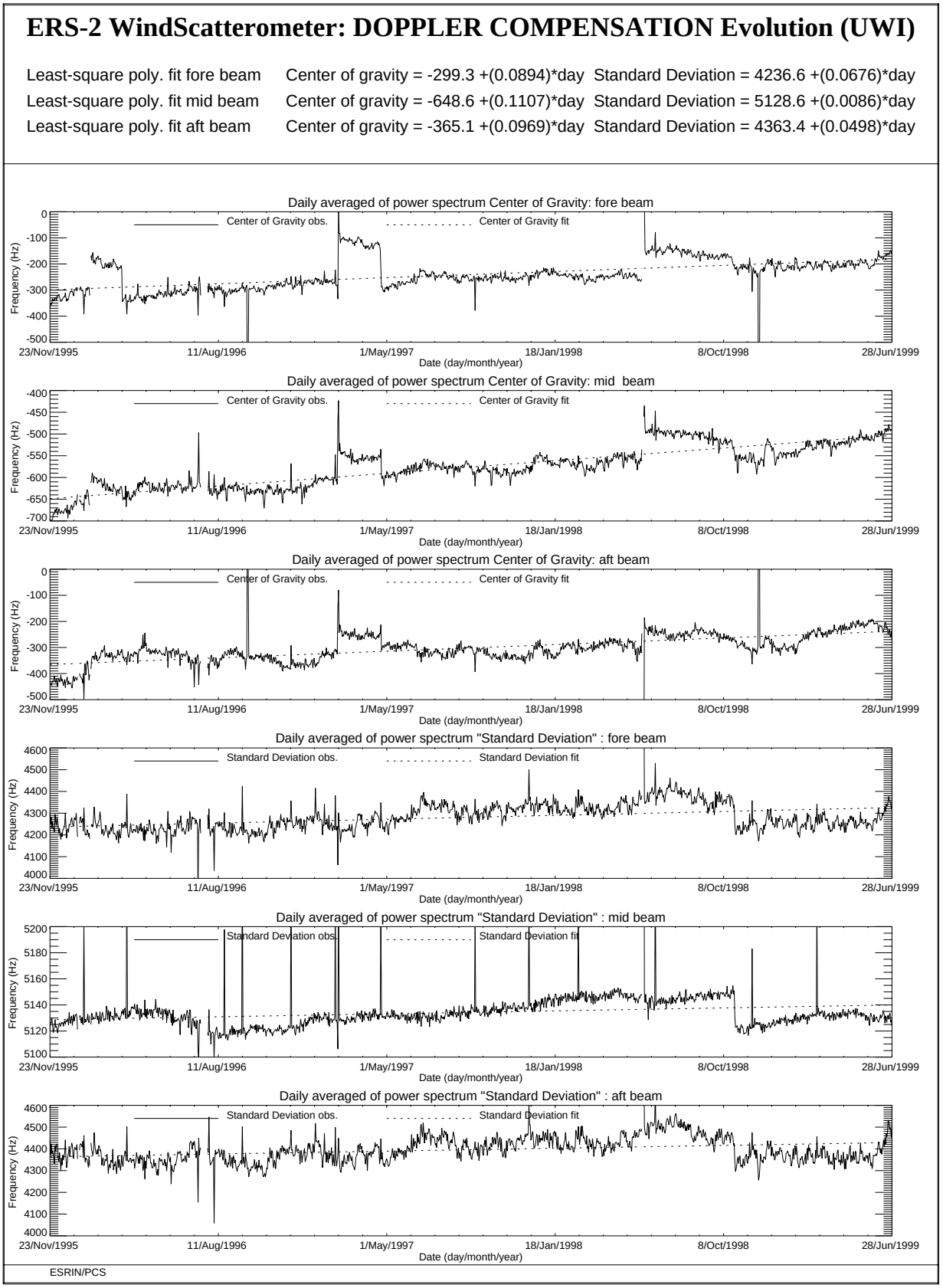

FIGURE 16. ERS-2 Scatterometer: Centre of Gravity and standard deviation of received power spectrum since the beginning of the mission.

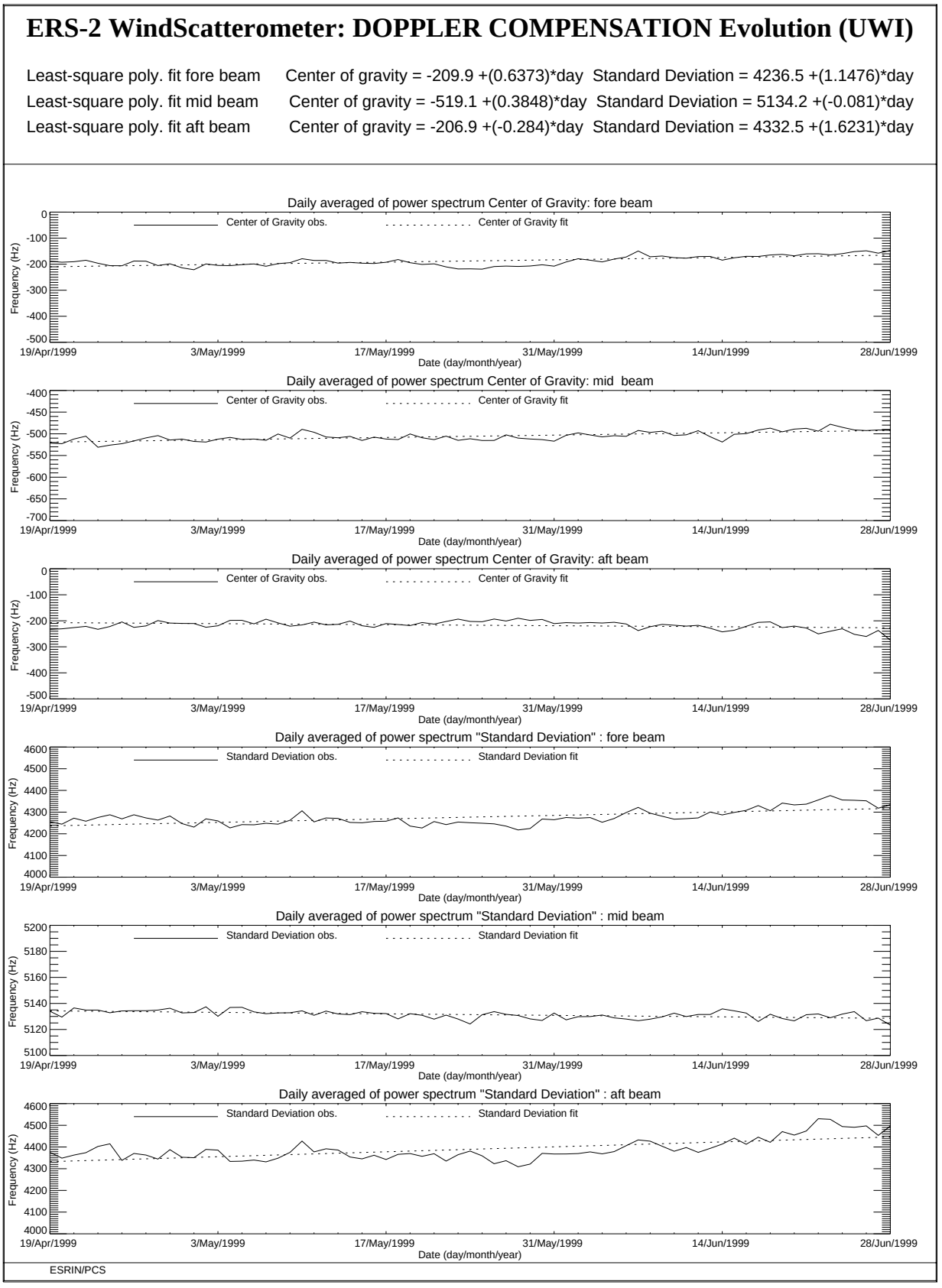

FIGURE 17. ERS-2 Scatterometer: Centre of Gravity and standard deviation of received power spectrum cycle 42 and cycle 43.

3.2 Noise power level I and Q channel

The results of the monitoring are shown in Figure 18. The first set of three plots presents the noise power evolution for the I channel while the second set shows the Q channel. The noise level is less than 1 ADC Unit for the fore and aft signals and is negligible for the mid one. From the plots one can see that the noise level is more stable in the I channel than in the Q one. The PCS suspects that an explanation should be found in the different position of the receivers, in particular it seems that the Q one is closer to the ATSR-GOME electronics. A confirmation of this hypothesis has been asked to ESTEC.

Since 5th December 1997 some high peaks appear in the plots. These high values for the daily mean are due to the presence for these special days of a single UWI product with an unrealistic value in the noise power field of the Specific Product Header. The analysis of the raw data used to generate these products lead in all cases to the presence of one source packet with a corrupted value in the noise field stored into the source packet Secondary Header. Table 4 presents the list of the UWI products affected by a corrupted noise field and disseminated during cycle 43.

Table 4: UWI products with noise field corrupted (cycle 43)

Noise Field corrupted	Noise value (ADC Unit)	Acquisition Time
None	-	-

The reason why noise field corruption is beginning from 5th December 1997 is at present unknown. It is interesting to note that at the beginning of December 1997, we started to get as well the corruption of the Satellite Binary Times (SBTs) stored in the EWIC product. The impact in the fast delivery products was the production of blank products starting from the corrupted EWIC until the end of the scheduled stop time. A change in the ground station processing in March 1998 overcame this problem.

Since 9th August 1998 some periods with a clear instability in the noise power have been recognised. Table 5 gives the detailed list.

Table 5: ERS-2 Scatterometer instability in the noise power

From	To
9th August 1998	26th October 1998
29th November 1998	6th December 1998
23rd December 1998	24th December 1998
7th June 1999	10th June 1999

To better understand the instability of the noise power the PCS has carried out investigations in the scatterometer raw data (EWIC) to compute the noise power with more resolution. The result is

that for the orbits affected by the instability the noise power had a decrease of roughly 0.7 dB for the fore and aft signals and a decrease of roughly 0.6 dB in the mid beam case (see report cycle 42). The decrease of the noise power during the orbits affected by the instability is comparable with the decrease of the internal calibration level that occurred during the same orbits. The reason of this instability (linked to the AMI anomalies) is still under investigation. The correlation among the noise power, the internal calibration level and the AMI anomaly is reported in section 3.3.

Figure 19 shows the evolution of the noise power since 26th October when 2 dB were added to the transmitted power.

During cycle 43 the evolution of the noise power was nominal, apart from the period from 7th June to 9th June (noise power instability in connection with the AMI anomaly).

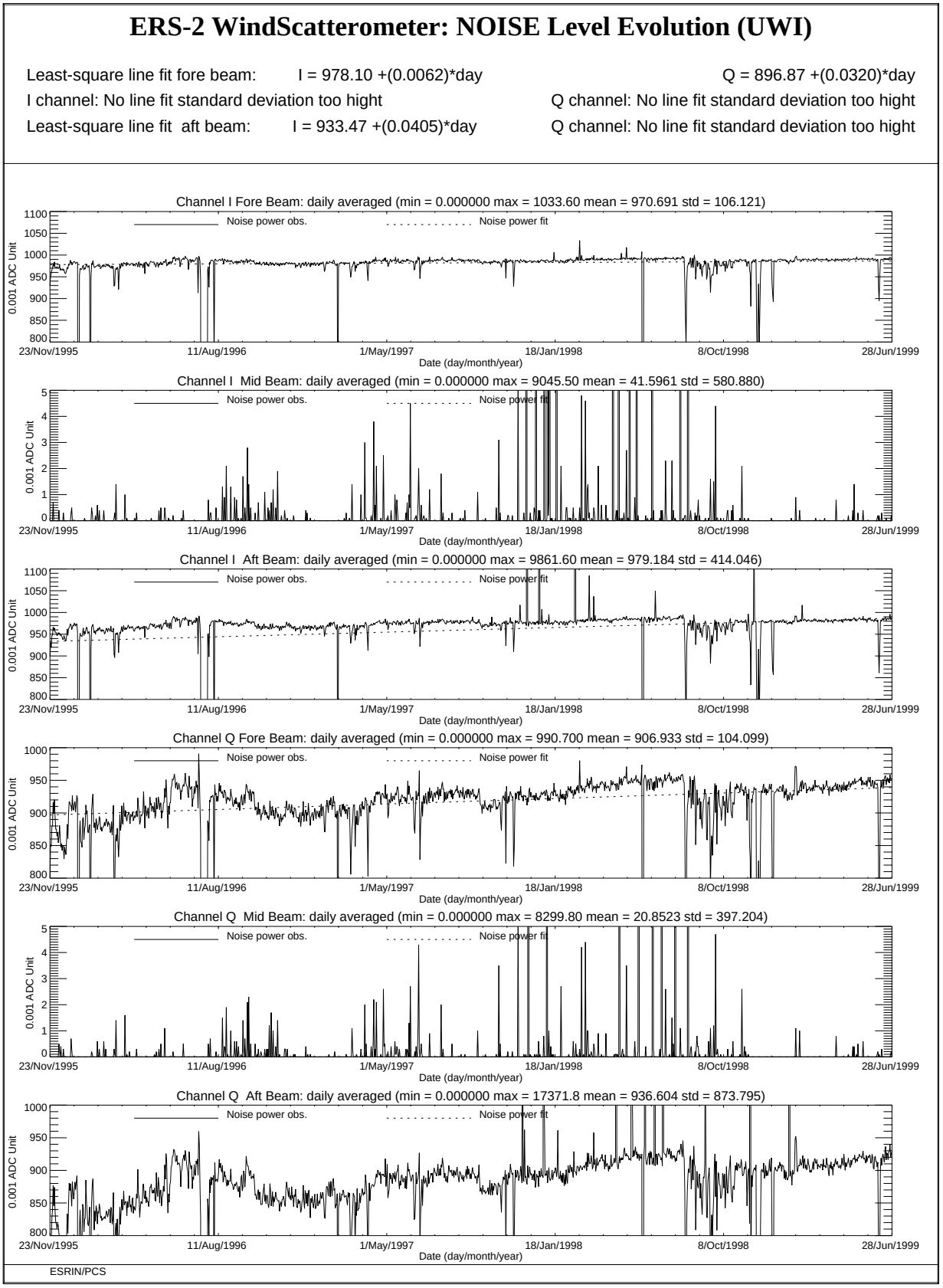

FIGURE 18. ERS-2 Scatterometer: noise power I and Q channel since the beginning of the mission.

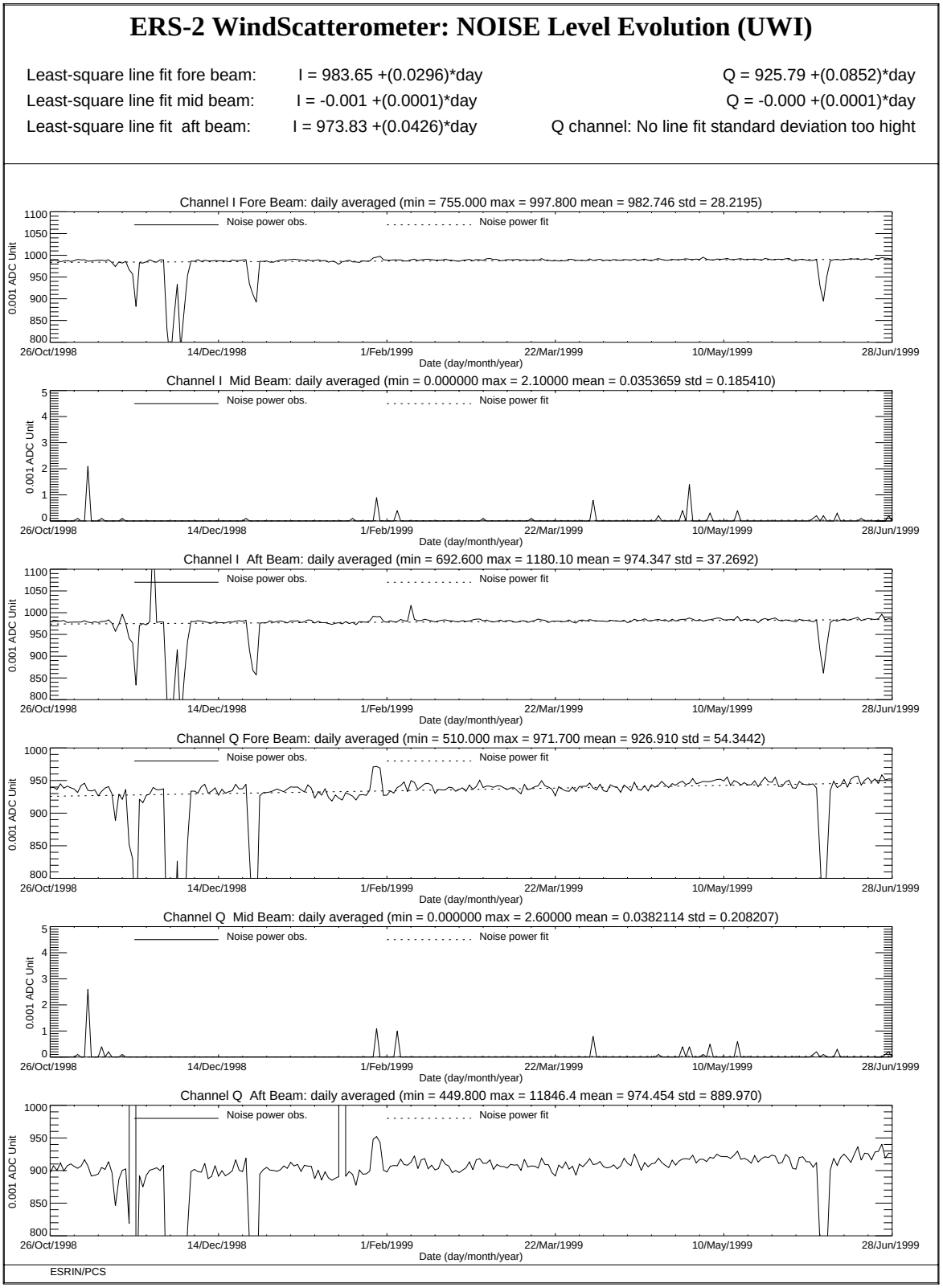

FIGURE 19. ERS-2 Scatterometer: noise power I and Q channel since 26th October 1998 when the transmitted power was increased by 2 dB.

3.3 Power level of internal calibration pulse

For the internal calibration level, the results, since the beginning of the mission, are shown in Figure 21.

The high value of the variance in the fore beam until August,12th 1996 is due to ground processing. In fact, all the blank source packets ingested by the processor were recognized as fore beam source packets with a default value for the internal calibration level. The default value was applicable for ERS-1 and therefore was not appropriate for ERS-2 data processing. On August 12th, 1996 a change in the ground processing LUT overcame the problem.

Since the beginning of the mission a power decrease is detected. The reason is that the TWT is not working in saturation, so that a variation in input signal is visible in output. The variability of the input signal can be two-fold: the evolution of the pulse generator or the tendency of the switches between the pulse generator and the TWT to reset themselves into a nominal position. These switches were set into an intermediate position in order to put into operation the scatterometer instrument (on 16th November 1995). The decrease is estimated to be about 0.0025 dB per day. After the change of the calibration subsystem on August 6th, 1996 the decrease is more evident and it is estimated in 0.1 dB per cycle. The power decrease is regular and affects the AMI when it is working in wind-only mode, wind/wave mode and image mode indifferently.

On 26th October 1998 to compensate for this decrease, 2.0 dB were added to the Scatterometer transmitted power and this explains the large step shows in Figure 20.

It is important to point out the efficiency of the internal calibration for keeping the absolute calibration level stable. In fact, no important change is noted in the monitoring of the gamma-nought level over the Brazilian rain forest during the power decrease and after the increase of the transmitted power (see section 2.0).

The internal calibration level shows an instability since 9th August 1998 that is very well correlated with the instability in the noise power outlined in section 3.2.

Figure 20 shows the daily average of the internal calibration and the noise power from 1st August 1998 to 26th June 1999. In the figure are also reported the anomalies that affected the AMI (the triangles in the plot) and the days when the instability was very strong (asterisks in the plot). From Figure 20 it seems that there is a correlation between the instability and the AMI anomalies. In fact the internal calibration level during the cycle 43 had a new period of instability from 7th June to 9th June 1999 in connection with the AMI anomaly occurred on 7th June 1999.

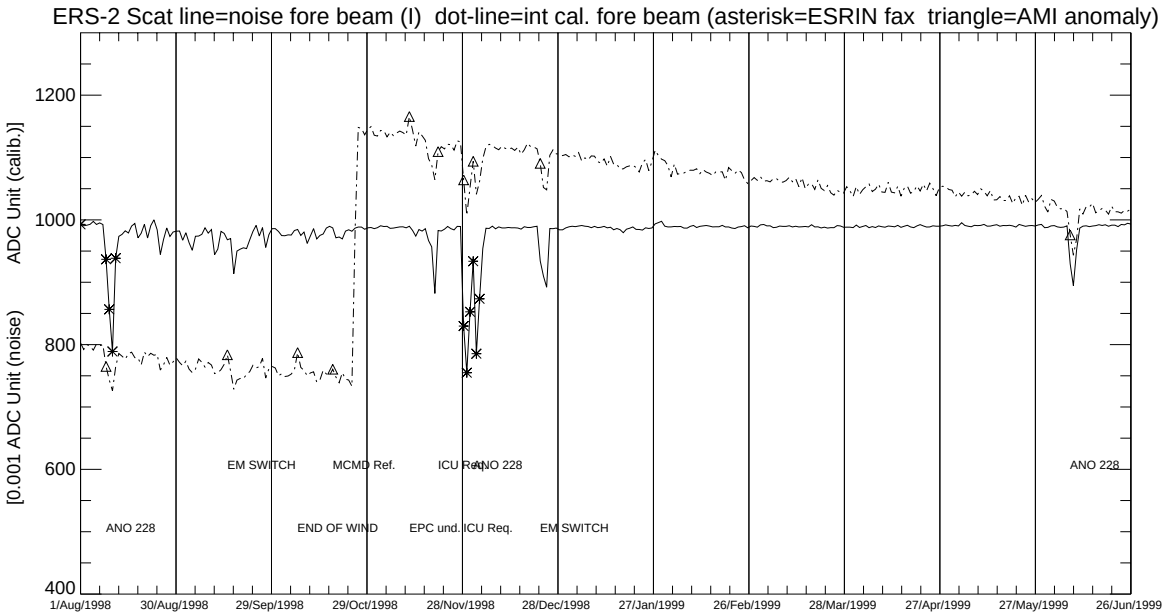

FIGURE 20. ERS-2 Scatterometer: noise power (I channel fore antenna) and internal calibration power (fore antenna) evolution from 1st August 1998 to 26th June 1999.

Figure 21 shows the evolution of the internal calibration level since 26th October 1998. From 26th October 1998 (cycle 37) to 28th June 1999 (cycle 43) the internal calibration level had a decrease, of roughly 0.5 dB (for the three antennae) on average 0.07 dB per cycle. This actual decrease is, on average, less than the one reported before the increase of the transmitted power (0.1 dB per cycle).

During the cycle 43 the power decrease was 0.1 dB. This result is very close to the one obtained for the previous cycle (0.09 dB).

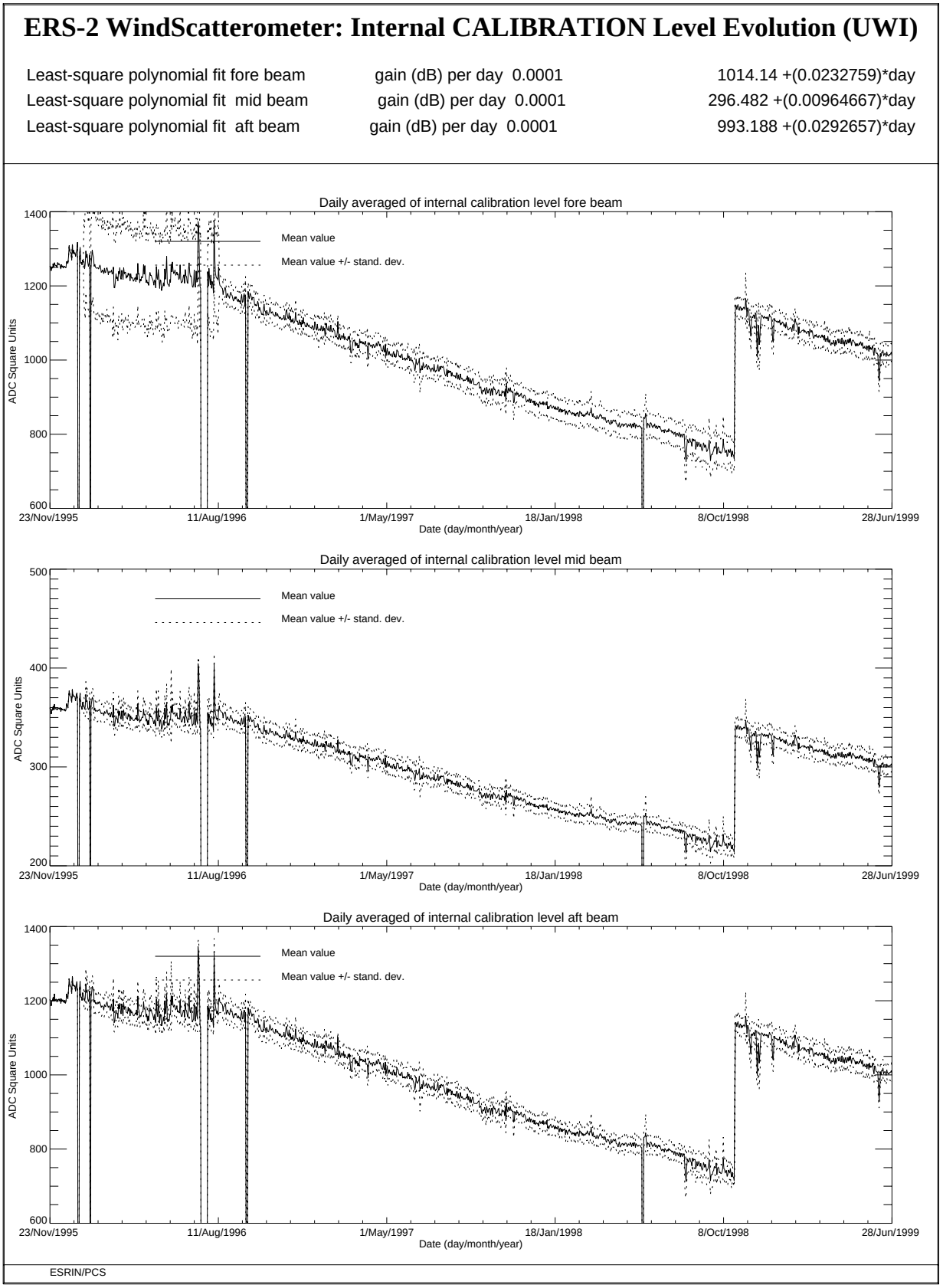

FIGURE 21. ERS-2 Scatterometer: power of internal calibration pulse since the beginning of the mission.

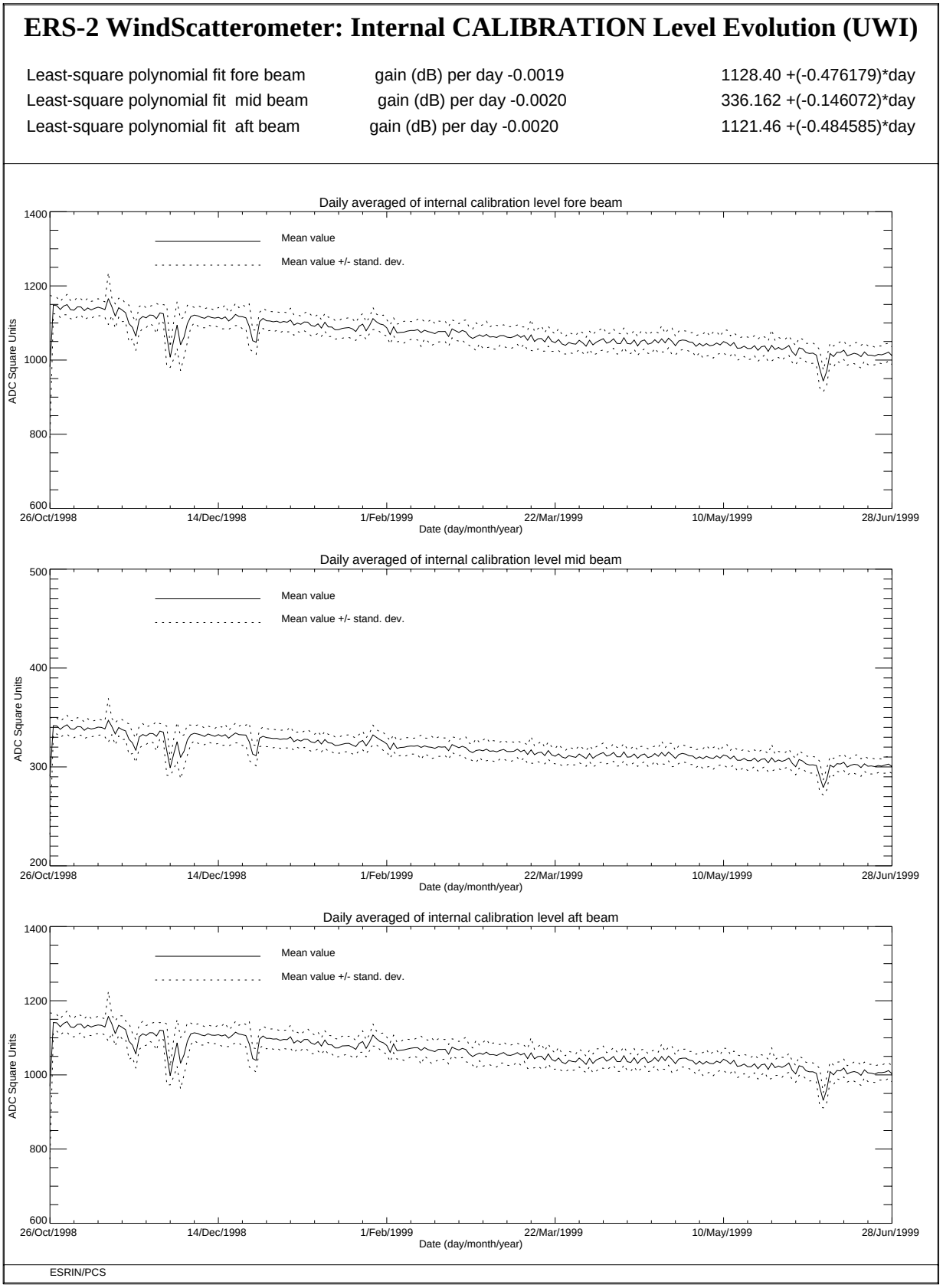

FIGURE 22. ERS-2 Scatterometer: power of internal calibration level since 26th October 1998 when the transmitted power was increased by 2.0 dB.

4.0 Products performance

One of the most important point in the monitoring of the products performance is their availability. The Scatterometer is a part of ERS payload and it is combined with a Synthetic Aperture Radar (SAR) into a single Active Microwave Instrument (AMI). The SAR users requirements and the constraints imposed by the on-board hardware (e.g. amount of data that can be recorded in the on-board tape) set rules in the mission operation plan.

The principal rules that affected the Scatterometer instruments are:

- over the Ocean the AMI is in wind/wave mode (scatterometer with small SAR imagettes acquired every 30 sec.) and the ATSR-2 is in low rate data mode.
- over the Land the AMI is in wind only mode (only scatterometer) and the ATSR-2 is in high rate mode. (Due to on board recorder capacity, ATSR-2 in high rate is not compatible with Sar wave imagette acquisitions.)

This strategy preserves the Ocean mission.

Moreover:

- the SAR images are planned as consequence of users' request.

These rules have an impact on the Scatterometer data availability as shown in Figure 23.

Each segment of the orbit has different colour depending on the instrument mode: brown for wind only mode, blue for wind-wave mode and green for image mode. The red and yellow colours correspond to gap modes (no data acquired). The major problems came from the orbit segments between Australia and Antarctic and between Africa and Antarctic where a lot of data are not acquired. This problem is under investigation by ESRIN and a new mission operation plan for the scatterometer shall be adopted.

For cycle 43 the percentage of the ERS-2 AMI activity is shown in table 6.

Table 6: ERS-2 AMI activity (cycle 43)

AMI modes	ascending passes	descending passes
Wind and Wind-Wave	**89.3%**	**82.0%**
Image	**2.5%**	**8.0%**
Gap and others	**8.2%**	**10.0%**

During the cycle 43 there was an improvement in the scatterometer coverage of the west coast of the Mexico at descending passes. The west coast of Mexico is an important area to monitoring the formation of the tropical cyclones and scatt data are very useful into the forecast of these natural events (as reported by the ASCATT-SAG members). The improvement is due to the reduction of the length of the SAR segment acquired over the east coast of the USA. The length of the SAR images, over the east coast of USA, are now strictly limited to the length requested by the users.

Table 7 reports the major data lost due to the test periods and AMI or satellite anomalies occurred after August 6th, 1996 (before of this day for many times data were not acquired due to the DC converter failure).

Table 7: ERS-2 Scatterometer mission major data lost after 6th, August 1996

From	To	Reason
September 23rd, 1996	September 26th, 1996	Test period
February 14th, 1997	February 15th, 1997	Depointing anomaly
June 3rd, 1998	June 6th, 1998	Depointing anomaly
November 17th, 1998	November 18th, 1998	ERS-2 switched off to face out Leonide meteo storm

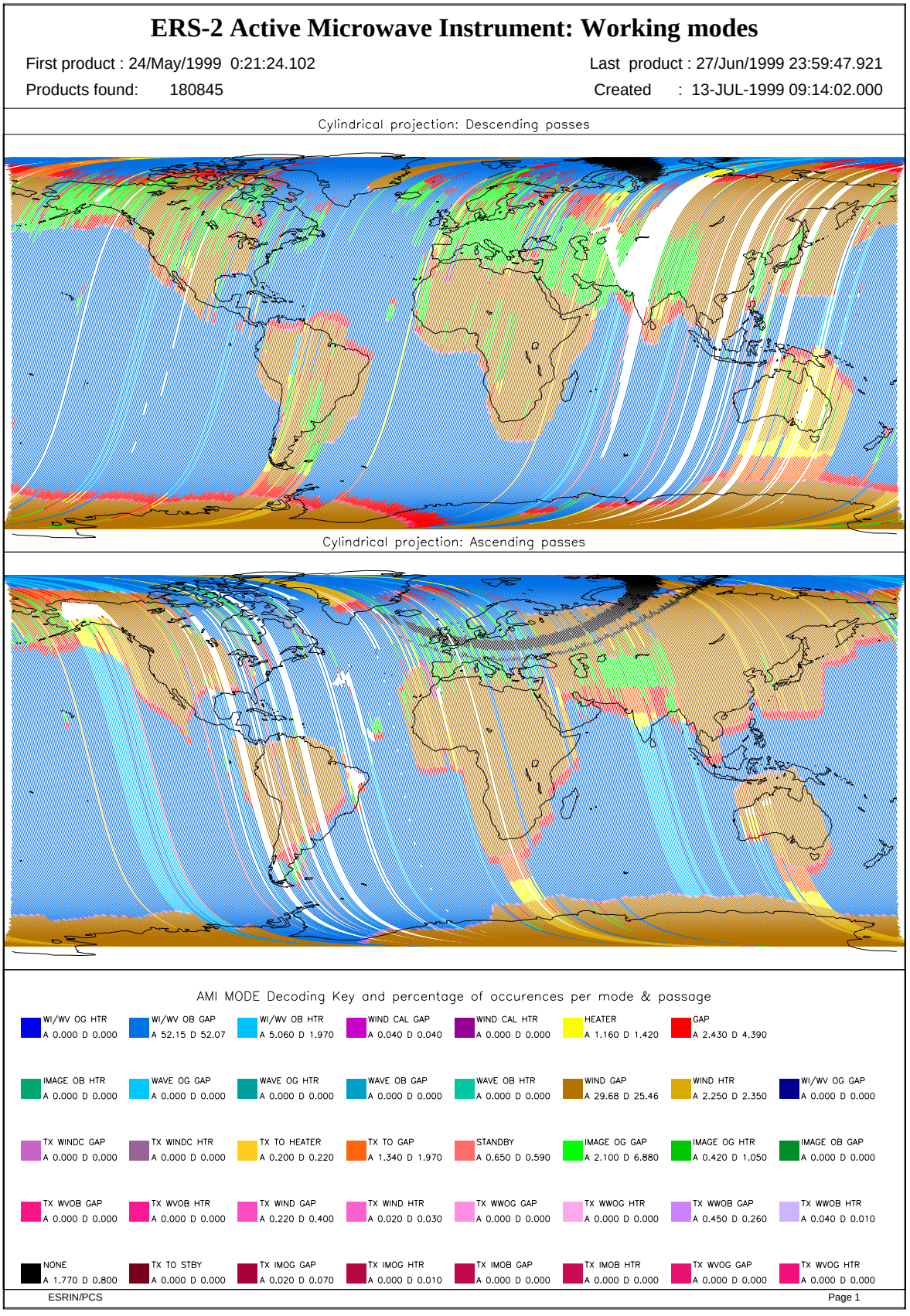

FIGURE 23. ERS-2 AMI activity during cycle 43

The PCS carries out a quality control of the winds generated from the WSCATT data. The activity is split in two main areas: the first one includes a routine analysis of the fast Delivery Products disseminated to the users, the second one is focused on the improvement of the CMOD-4 (the operative ESA wind retrieval algorithm) for high wind speed. External contributions to this quality control come also from ECMWF and UK-Met Office.

The routine analysis is summarized in the plots of figure 24; from top to bottom:

- the monitoring of the valid sigma-nought triplets per day.
- the evolution of the wind direction quality. The ERS wind direction (for all nodes and only for those nodes where the ambiguity removal has worked properly) is compared with the ECMWF forecast. The plot shows the percentage of nodes for which the difference falls in the range -90.0, +90.0 degrees.
- the monitoring of the percentage of nodes whose ambiguity removal works successfully.
- the comparison of the wind speed deviation: (bias and standard deviation) with the ECMWF forecast.

The results since the beginning of the mission can be summarized as a stable number of valid sigma-nought after on August 6th, 1996 (apart from the events given in Table 7), an accurate wind direction for roughly 93% of the nodes, a success in the ambiguity removal for more than 90.0% of the nodes.

The ERS-2 wind speed shows an absolute bias of roughly 0.5 m/s and a standard deviation that ranges from 2.5 m/s to 3.5 m/s with respect to the ECMWF forecast. This standard deviation has a seasonal pattern due to the different winds distribution between the winter and summer season.

It is important to note that only after the end of calibration phase (mid March 1996) the wind products have reached high quality.

Two important changes affect the speed bias plot: the first is on June 3rd, 1996 and it is due to the switch from ERS-1 to ERS-2 data assimilation in the meteorological model. The second change, which occurred at the beginning of September 1997, is due to the new monitoring and assimilation scheme in ECMWF algorithms (4D-Var).

Since 19th April 1999 two set of meteo-table (meteorological forecast centred at 00:00 and 12:00 of each day) are used in the ground processing. With this new strategy the data are processed using the 18 and 24 hours meteorological forecast instead of the 18, 24, 30 36 hours forecast. The data processed with the 18-24 hours tables instead of 30-36 hours tables have an increase in the number of ambiguity removed nodes but no important improvements are shown, on average, in the daily statistics.

For cycle 43 the PCS quality control has reported stable results apart from the day 21st June 1999 when the operational set of meteo tables was missing into the ground station of Gatineau. This caused an ambiguity removal rate around 82% for that day.

The ECMWF reports, attached as annex, presents stable performances in the monitoring of the ERS-2 wind for the cycle 43. The wind speed bias is roughly -0.43 m/s for the UWI-FG analysis and -0.17 m/s for the FG-4D-Var case with a standard deviation of 1.56 m/s (UWI-FG) and 1.67 m/s (FG-4D-Var). The wind direction standard deviation is between 30 and 65 degrees (UWI -

FG) or 15 and 30 degrees (FG-4D-Var). These results are very similar to the ones obtained in the previous report.

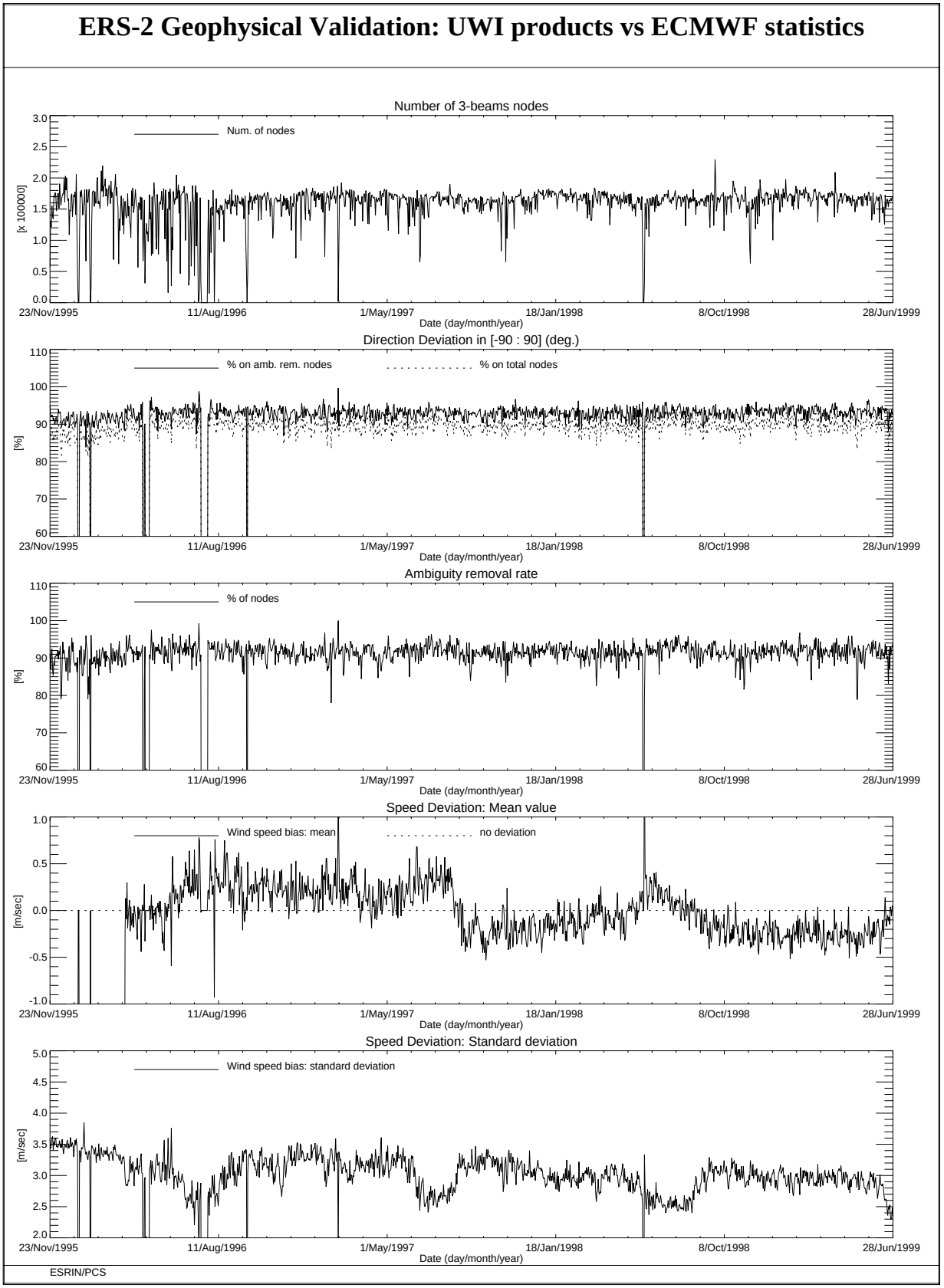

FIGURE 24. ERS-2 Scatterometer: wind products performance since the beginning of the mission.